

## Structure-Based Design of Human TLR8-Specific Agonists with Augmented Potency and Adjuvanticity

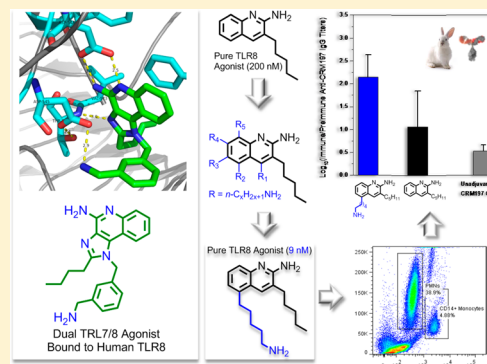
Mallesh Beesu,<sup>†</sup> Giuseppe Caruso,<sup>†</sup> Alex C. D. Salyer,<sup>†</sup> Karishma K. Khetani,<sup>†</sup> Diptesh Sil,<sup>†</sup> Mihiri Weerasinghe,<sup>†</sup> Hiromi Tanji,<sup>‡</sup> Umeharu Ohto,<sup>‡</sup> Toshiyuki Shimizu,<sup>‡</sup> and Sunil A. David<sup>\*,†</sup>

<sup>†</sup>Department of Medicinal Chemistry, University of Kansas, Lawrence, Kansas 66047, United States

<sup>‡</sup>Graduate School of Pharmaceutical Sciences, University of Tokyo, Tokyo 113-0033, Japan

### S Supporting Information

**ABSTRACT:** Human Toll-like receptor 8 (hTLR8) is expressed in myeloid dendritic cells, monocytes, and monocyte-derived dendritic cells. Engagement by TLR8 agonists evokes a distinct cytokine profile which favors the development of type 1 helper T cells. Crystal structures of the ectodomain of hTLR8 cocrystallized with two regioisomers of a dual TLR7/8-agonistic N1-substituted imidazoquinolines showed subtle differences in their interactions in the binding site of hTLR8. We hypothesized that the potency of a previously reported best-in-class pure TLR8 agonist, 3-pentylquinoline-2-amine, could be further enhanced by “designing in” functional groups that would mimic key intermolecular interactions that we had observed in the crystal structures. We performed a focused exploration of decorating the quinoline core with alkylamino groups at all possible positions. These studies have led to the identification of a novel TLR8 agonist that was ~20-fold more potent than the parent compound and displays prominent adjuvantic activity in a rabbit model of immunization.



## INTRODUCTION

The Centers for Disease Control and Prevention (CDC) has declared vaccination and the control of infectious diseases to be among the greatest public health achievements of the 20th century.<sup>1</sup> Vaccines afford protection by the induction of immune responses, both humoral and cellular, specifically directed against the pathogen. A significant trend in contemporary vaccinology is the design of highly effective subunit vaccines, and the majority of modern subunit vaccines that utilize highly purified, recombinantly expressed protein immunogens are reliant on vaccine adjuvants<sup>2,3</sup> (substances that enhance immune responses) to provide the initial, innate immune-activating signals that determine the specificity, magnitude, quality, and durability of downstream adaptive immune responses.

With few exceptions, the majority of currently available vaccines contain a single adjuvant: “alum” introduced by Alexander Glennie in 1926.<sup>4</sup> “Alum” (a mixture of aluminum phosphate and aluminum hydroxide) appears to promote a T helper 2 (Th2) skewed antibody response.<sup>5,6</sup> Indeed, alum-adjuvanted pertussis subunit vaccines,<sup>7</sup> which supplanted killed whole-cell pertussis vaccines in the 1990s, induce immunity that rapidly wanes;<sup>8–10</sup> the short-lived immunity is thought to contribute to the recent re-emergence of pertussis in the United States<sup>11,12</sup> and elsewhere in the world.<sup>13,14</sup> In experimental models of pertussis, alum-adjuvanted acellular pertussis vaccines protected baboons in the short term from severe pertussis-like symptoms but failed to prevent colonization of *B. pertussis*, allowing transmission of the pathogen to unvaccinated animals;<sup>15</sup> killed whole-cell pertussis vaccines, on the other hand, elicited strong *B. pertussis*-specific Th17 and Th1

memory,<sup>15</sup> indicating that both durability and quality of immune responses are pivotal in the induction and maintenance of long-term sterilizing immunity.

Innate immune signals evoked by vaccine adjuvants include those originating from Toll-like receptors (TLRs),<sup>16–18</sup> as well as RIG-I-like receptors<sup>19</sup> and NOD-like receptors (NLRs).<sup>20,21</sup> There are 10 functional TLRs encoded in the human genome, which are transmembrane proteins with an extracellular domain having leucine-rich repeats (LRR) and a cytosolic domain called the Toll/IL-1 receptor (TIR) domain.<sup>17</sup> The ligands for these receptors are highly conserved molecules such as lipopolysaccharides (LPS) (recognized by TLR4), lipopeptides (TLR2 in combination with TLR1 or TLR6), flagellin (TLR5), single stranded RNA (TLR7 and TLR8), double stranded RNA (TLR3), CpG motif-containing DNA (recognized by TLR9), and profilin present on uropathogenic bacteria (TLR11).<sup>17</sup> TLR1, -2, -4, -5, and -6 recognize extracellular stimuli, while TLR3, -7, -8, and -9 function within the endolysosomal compartment.

Our understanding of how the engagement of innate immune receptors by vaccine adjuvants leads to the deployment and amplification of immunogen-specific adaptive immune responses,<sup>16,17,22</sup> and the maintenance of immunological memory is incomplete and may involve multiple mechanisms and pathways; these may include (i) enhanced antigen uptake and presentation by professional antigen presenting cells

Received: July 12, 2015

Published: September 9, 2015

(APCs),<sup>23–30</sup> (ii) amplification of cross-talk<sup>31–33</sup> between naive B lymphocytes recognizing the immunogen and rare naive CD4<sup>+</sup> T cells expressing T cell antigen receptors (TCRs) specific for antigen-derived peptide/major histocompatibility complex class II molecules (MHCII) displayed by such naive B cells, (iii) accelerated differentiation of CD4<sup>+</sup> T cells into follicular helper T cells (T<sub>fh</sub>),<sup>34–37</sup> and (iv) subsequent B lymphocyte differentiation events leading to immunoglobulin affinity maturation<sup>38,39</sup> and the generation of antigen-specific memory B cells and plasma cells.<sup>40–42</sup>

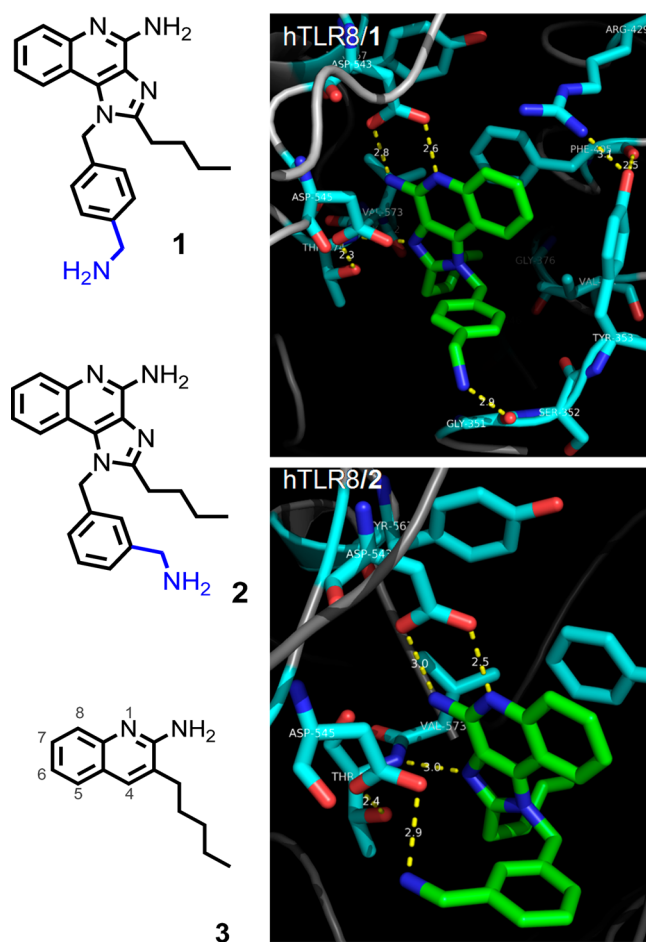
The need for the development of safe and effective vaccine adjuvants has fueled our exploration of a variety of innate immune stimuli, which include agonists of TLR2,<sup>43–45</sup> TLR7,<sup>46–54</sup> TLR8,<sup>54–59</sup> nucleotide oligomerization domain 1 (NOD1),<sup>60</sup> as well as C–C chemokine receptor type 1 (CCR1).<sup>61</sup> Structure–activity relationship studies have proven useful in providing tools with which to examine how these different classes of innate immune signaling molecules affect and modulate pathways linking the innate and adaptive immune systems described above.

TLR8 is expressed predominantly in myeloid dendritic cells, monocytes, and monocyte-derived dendritic cells.<sup>62,63</sup> Engagement by TLR8 agonists evokes a dominant proinflammatory cytokine profile, including tumor necrosis factor  $\alpha$  (TNF- $\alpha$ ), interleukin (IL)-12, and IL-18 and appear uniquely potent in enhancing the production of Th1-polarizing cytokines TNF- $\alpha$  and IL-12 in APCs.<sup>62,64–66</sup> Our interest in small molecule agonists of TLR8 has led to the exploration of the 2,3-diaminofuro[2,3-*c*]pyridines,<sup>55</sup> 4-aminofuro[2,3-*c*]quinolines,<sup>57</sup> 3-alkylquinoline-2-amines,<sup>58</sup> and 1-alkyl-2-aminobenzimidazoles,<sup>59</sup> all of which are pure TLR8 agonists with no detectable activity at TLR7.

Crystal structures of the ectodomain of human TLR8 (hTLR8) cocrystallized with two regioisomers of dual TLR7/8-agonistic *N*<sup>1</sup>-aminomethylbenzyl-substituted imidazoquinolines<sup>47</sup> (**1**, **2**) showed subtle differences in their interactions in the binding site of hTLR8 (Figure 1). The *N*<sup>1</sup>-substituent of **1** was observed to H-bond with a backbone carbonyl group, while in **2**, a stronger salt-bridge was present, which fully explained the higher TLR8 activity of **2**. We sought to apply these findings and asked whether the TLR8-agonistic potency of the best-in-class compound of the 3-alkylquinoline-2-amine series<sup>58</sup> could be further enhanced by “designing in” functional groups which would mimic the ionic H-bond observed in the hTLR8/2 complex. We now report a focused and hypothesis-driven exploration of introducing alkylamino groups at all possible positions on the quinoline core. These studies led to the identification of a novel TLR8 agonist which was ~20-fold more potent than the parent compound.

## RESULTS AND DISCUSSION

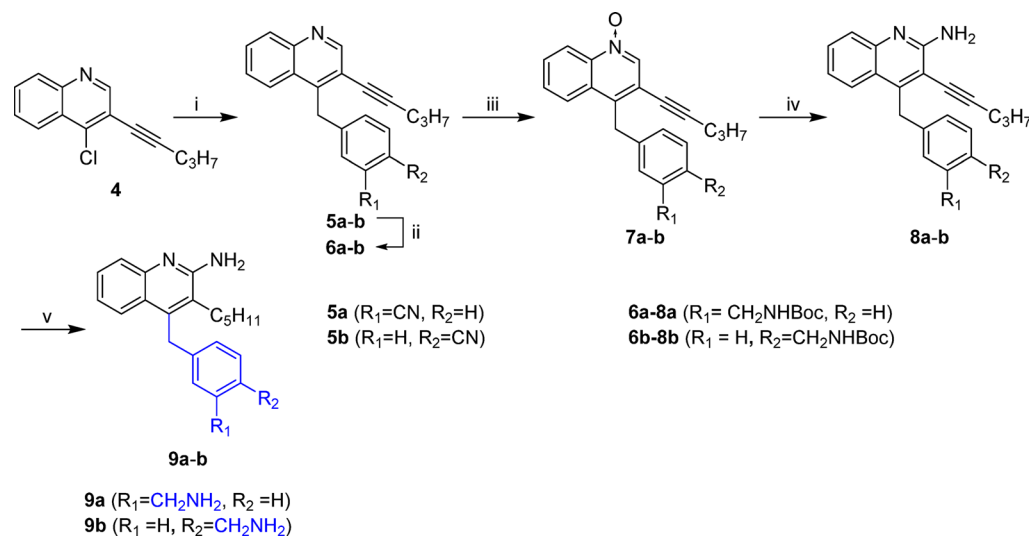
The dual TLR7/8-active regioisomeric imidazoquinolines **1** and **2** (Figure 1), synthesized when we first began our investigations on TLR-active compounds,<sup>47</sup> showed substantially different agonistic potencies in human TLR7 (**1**, 50 nM; **2**, 215 nM) and TLR8 (**1**, 55 nM; **2**, 14 nM) primary screens (Figure S1 in Supporting Information). The crystal structures of these two congeners bound to the ectodomain of human TLR8 reveal the structural basis of enhanced TLR8-agonistic potency of **2** relative to **1**: the 3-aminomethylbenzyl substituent in **2** forms a strong ionic H-bond (salt bridge) with the side chain carboxylate of Asp545, while the 4-aminomethylbenzyl substituent in **1** is observed to engage the backbone carbonyl of Gly351 in a weaker H-bond (Figure 1). The stronger interaction of **2** in its



**Figure 1.** Left: structures of the dual TLR7/8-active *N*<sup>1</sup>-4-aminomethylbenzyl (**1**) and *N*<sup>1</sup>-3-aminomethylbenzyl (**2**) substituted imidazoquinolines and pure TLR8-agonistic 3-pentylquinolin-2-amine (**3**). Right: Crystal structures of **1** and **2** bound to human TLR8. Dashed lines in yellow depict direct hydrogen bonds.

binding site resulted not only in enhancement of agonistic activity in primary screens (Figure S1) but also in higher proinflammatory cytokine induction in whole human blood assays (data not shown). The 3-pentylquinoline-2-amine **3**, derived from structure-based ligand design, had previously been identified as a human TLR8-specific agonist ( $EC_{50} = 200$  nM).<sup>58</sup>

We asked whether grafting the aminomethylbenzyl group on to the 3-pentylquinoline-2-amine moiety would result in augmented activity. Direct  $S_NAr$  displacement of the 4-chloro-3-(pent-1-yn-1-yl)quinoline intermediate<sup>58</sup> **4** with 3- or 4-cyanobenzylzinc bromide as nucleophile<sup>67</sup> afforded the 4-substituted 3-pentynylquinolines **5a** and **5b** (Scheme 1); reduction of the nitriles with  $LiAlH_4$  and subsequent Boc protection of the resultant amines yielded the intermediates **6a** and **6b**. Installation of the amine at C2 was performed as reported earlier.<sup>58</sup> Hydrogenation of the alkynyl group and Boc-deprotection furnished the desired target compounds **9a** and **9b** (Scheme 1) which retained specificity for TLR8 but with marginal improvement in potency (150 and 120 nM, respectively; Table 1). In order to examine relieving possible steric bulk of the aminomethylbenzyl substituent at C4, we undertook the synthesis of the 4-aminobutyl (**14a**) and 5-aminopentyl (**14b**) analogues (Scheme 2), the lengths of which were found to be optimal in SAR studies on several TLR8-active chemotypes.<sup>54,55,57–59</sup> Installation of the 4-alkylnitrile groups of

Scheme 1<sup>a</sup>

<sup>a</sup>Reagents: (i) 3-cyanobenzylzinc bromide (for **5a**) or 4-cyanobenzylzinc bromide (for **5b**), LiCl, DMF; (ii) (a) LiAlH<sub>4</sub>, THF, (b) Boc<sub>2</sub>O, CH<sub>3</sub>OH; (iii) *m*-CPBA, CHCl<sub>3</sub>; (iv) (a) benzoyl isocyanate, CH<sub>2</sub>Cl<sub>2</sub>, (b) NaOCH<sub>3</sub>, CH<sub>3</sub>OH; (v) (a) Pt/C, EtOAc, 30 psi, (b) HCl, 4 M.

**10a,b** was carried out with cyanoalkylzinc bromides under Negishi conditions (Scheme 2), and the remainder of the sequence of reactions was similar to those described in Scheme 1. The potencies of **14a** and **14b** remained virtually unchanged (190 and 250 nM, respectively; Table 1).

Our first attempts at attaching amine-bearing appendages on the quinoline core at C4 to allow for additional salt-bridge interactions with Asp545 appeared unfruitful, and we set out to systematically examine substitutions at all other positions. We desired an efficient synthetic strategy to access 5-, 6-, 7-, and 8-substituted 2-amino-3-pentylquinolines. A one-pot method for the syntheses of 2-aminoquinoline-3-carboxamides has been reported using 2-aminobenzaldehyde and active methylene-group-bearing cyanoacetamides.<sup>68</sup> We envisioned that a modified Friedländer synthesis of key bromo-substituted 2-amino-3-pentylquinolines could be directly obtained via condensation–cyclization reactions of 2-aminobromobenzaldehydes with heptanenitrile. Our initial attempts at model reactions with alkane nitriles and the unsubstituted 2-aminobenzaldehyde proceeded very well in the presence of *n*-butyllithium. However, in order to preempt possible debromination, we sought alternatives and successfully utilized potassium *tert*-butoxide to generate the pivotal bromo-substituted 2-amino-3-pentylquinolines (Schemes 3–7).

We targeted 2-amino-3-pentylquinolines substituted at C5 with 3-aminomethylbenzyl (**18a**), 4-aminomethylbenzyl (**18b**), and 2-aminomethylbenzyl (**18c**) substituents, which were obtained by Negishi coupling of corresponding cyanobenzylzinc bromides with **16** (Scheme 3). Substantially improved potencies were observed for both **18a** and **18b** (EC<sub>50</sub> of 49 and 38 nM, respectively; Figure 2, Table 1), whereas the 2-aminomethylbenzyl-substituted **18c** was significantly weaker (EC<sub>50</sub> = 1000 nM; Table 1) than the parent compound, **3**, suggesting that the placement of the amine on the benzyl substituent was an important determinant of activity. In order to formally test whether the amine was participating in the predicted salt bridge, the nitrile **17a** was hydrolyzed to the carboxamide analogue **18d** (Scheme 3). Compound **18d** and the 5-benzyl analogue **17d** were found to be inactive (Table 1), lending support to our hypothesis.

We next explored the role of conformational flexibility of the aminomethylbenzyl substituent at C5, and we therefore synthesized the aryl–aryl coupled 5-(aminomethyl)phenyl analogues **20a** and **20b** via Suzuki reaction of cyanophenylboronic acids with **16** (Scheme 4). Compound **20a** was entirely inactive, and the activity of **20b** was attenuated (699 nM), strongly pointing to the indispensability of conformational freedom. These findings prompted us to synthesize 5-aminoalkyl analogues (Schemes 5 and 6). The aminobutyl (**34a**), aminopentyl (**34b**), and aminohexyl (**34c**) derivatives could be accessed via Negishi couplings (Scheme 6); the reactivity of 2-cyanoethylzinc bromide with **16**, however, was very poor even under microwave conditions, and the aminopropyl analogue **23** was accessed via Heck reaction of acrylonitrile with **16** (Scheme 5). A clear dependence on the length of the alkylamine substituent was observed in these homologues with progressive increases in potency from the aminopropyl (**23**, 91 nM), aminobutyl (**34a**, 27 nM; Figure 2) and aminopentyl (**34b**, 9 nM; Figure 2) analogues; a further increase in length (**34c**, aminohexyl) led to decreased activity (56 nM, Table 1). Conversion of the nitrile precursor **30a** to the carboxamide derivative **34d** (Scheme 6) resulted in a dramatic decrease in potency (2181 nM, Table 1), once again highlighting the importance of the presence of a free amino functional group.

The dramatic enhancement of potency in **34b** seemed to unambiguously support our hypothesis of a salt-bridge between Asp545 and the 5-aminopentyl group of the lead compound. Given that guanidine–carboxylate interaction in proteins are consequential<sup>69,70</sup> and significant gains in interaction energies are observed in drugs such as zanamivir and peramivir whose crystal structures show strong salt-bridges between their guanidinium functional groups and the Asp/Glu residues that they interact with,<sup>71</sup> we synthesized from **34a** the guanidine derivative **34e** (Scheme 6), the length of the C5 substituent of which was calculated to be comparable to that of **34b**. We found, to our surprise, a precipitous fall in activity (2862 nM, Table 1), the reasons for which are yet to be understood.

We also explored aminoalkyl substitutions at C6 (**35a–c**), C7 (**36a–c**), and C8 (**37**) (Scheme 6). Compounds **35a–c** showed slight decreases in activity while analogues **36a–c**

Table 1. EC<sub>50</sub> Values of Compounds in Human TLR8-Specific Reporter Gene Assays

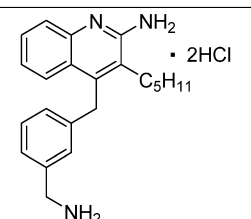
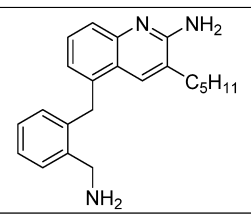
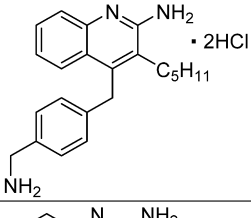
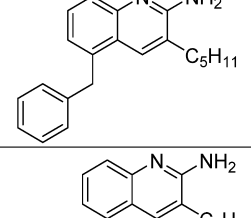
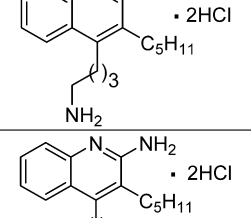
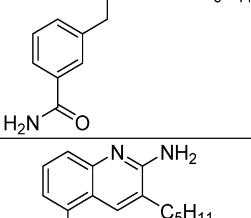
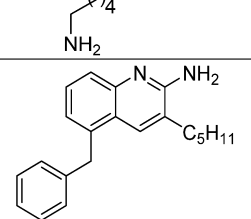
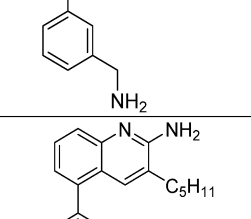
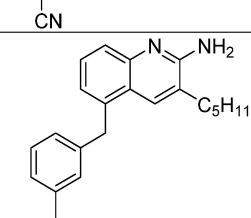
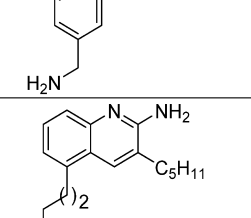
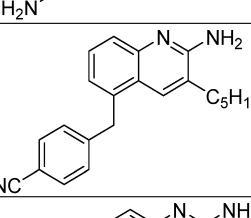
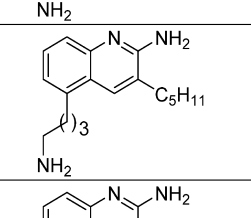
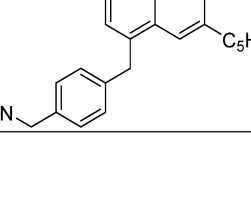
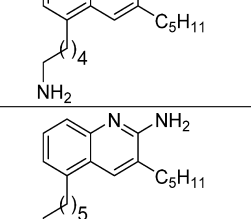

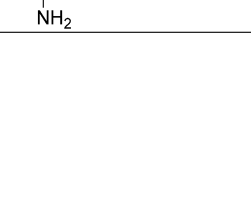

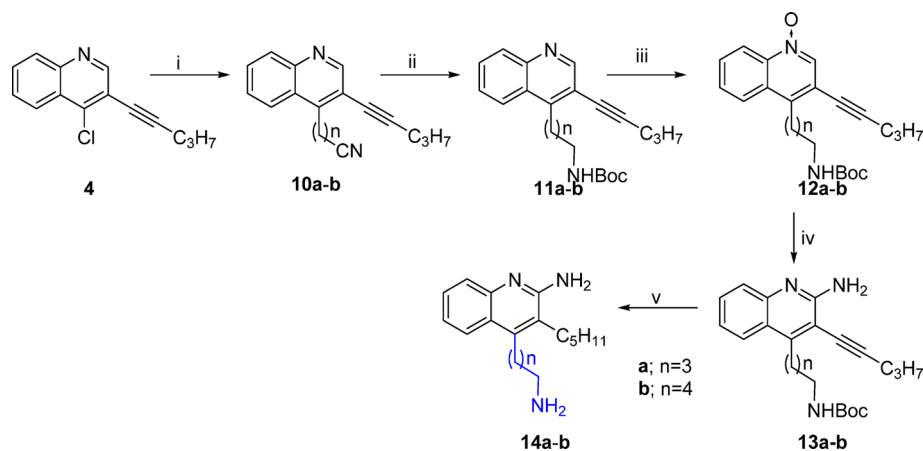
S. No.	Structure	TLR8 Agonistic Activity (nM) <sup>a</sup>	S. No.	Structure	TLR8 Agonistic Activity (nM) <sup>a</sup>
9a		150	18c		1000
9b		120	17d		Inactive
14a		190	18d		Inactive
14b		250	20a		Inactive
17a		Inactive	20b		699
18a		49	23		91
17b		Inactive	34a		27
18b		38	34b		9
			34c		56

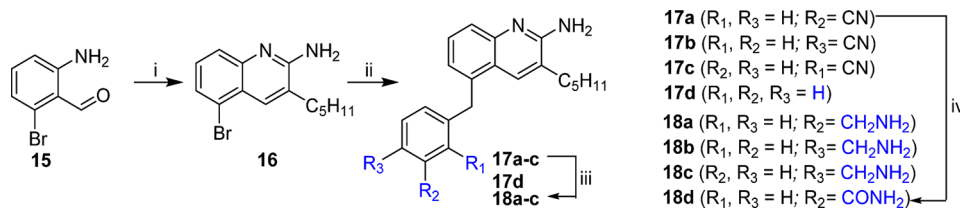
Table 1. continued

S. No.	Structure	TLR8 Agonistic Activity (nM) <sup>a</sup>	S. No.	Structure	TLR8 Agonistic Activity (nM) <sup>a</sup>
34d		2181	36a		60
			36b		50
34e		2862	36c		85
			37		Inactive
35a		727	43		621
35b		519			
35c		1016			

<sup>a</sup>EC<sub>50</sub> values represent the arithmetic mean values obtained on quadruplicate samples.

Scheme 2<sup>a</sup>

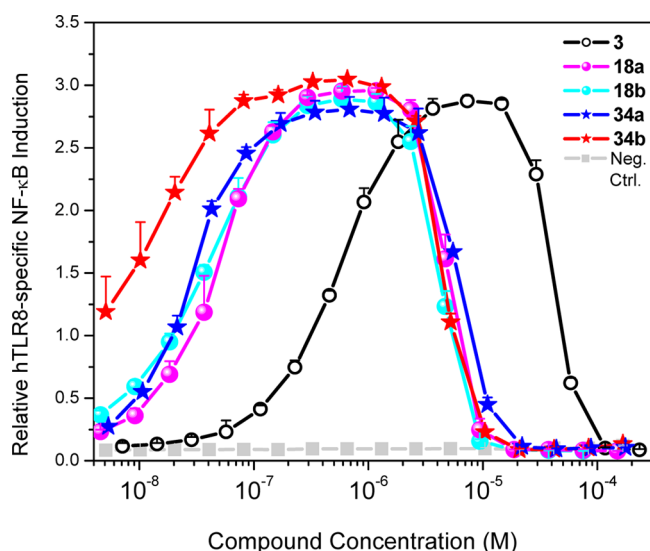
<sup>a</sup>Reagents: (i) 3-cyanopropylzinc bromide (for 10a) or 4-cyanobutylzinc bromide (for 10b), Pd(PPh<sub>3</sub>)<sub>4</sub>, THF; (ii) (a) LiAlH<sub>4</sub>, THF, (b) Boc<sub>2</sub>O, CH<sub>3</sub>OH; (iii) *m*-CPBA, CHCl<sub>3</sub>; (iv) (a) benzoyl isocyanate, CH<sub>2</sub>Cl<sub>2</sub>, (b) NaOCH<sub>3</sub>, CH<sub>3</sub>OH; (v) (a) Pt/C, EtOAc, 30 psi, (b) HCl, 4 M.

Scheme 3<sup>a</sup>

<sup>a</sup>Reagents: (i) heptanenitrile, *t*-BuOK, DMSO; (ii) 3-cyanobenzylzinc bromide (for 17a) or 4-cyanobenzylzinc bromide (for 17b) or 2-cyanobenzylzinc bromide (for 17c) or benzylzinc bromide (for 17d), Pd(PPh<sub>3</sub>)<sub>4</sub>, THF; (iii) LiAlH<sub>4</sub>, THF; (iv) KOH, *t*-BuOH, 8 h.

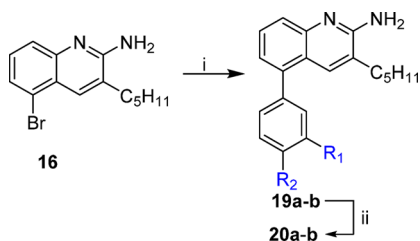
displayed modest gains in potency, with the most active compound being the 7-(5-aminopentyl)-3-pentylquinolin-2-amine, 36b (50 nM). The C8-substituted analogue 37 was

entirely devoid of activity (Table 1). Noting that the most potent analogues possessed an aminopentyl substituent either at C5 (34b, 9 nM) or C7 (36b, 50 nM), we wished to synthesize



**Figure 2.** Agonistic activities of analogues **18a**, **18b**, **34a**, and **34b** in human TLR8 reporter gene assays. Mean values  $\pm$  SD on quadruplicates are shown. Also included is **3**, used as a reference/comparator compound.

#### Scheme 4<sup>a</sup>



<sup>a</sup>Reagents: (i) 3-cyanophenylboronic acid (for **19a**) or 4-cyanophenylboronic acid (for **19b**), Pd(dppf)Cl<sub>2</sub>, K<sub>2</sub>CO<sub>3</sub>, 1,4-dioxane; (ii) LiAlH<sub>4</sub>, THF, 5 h.

a dually substituted analogue. The key precursor 2-amino-4,6-dibromobenzaldehyde was synthesized from 2-amino-4,6-dibromobenzoic acid using conventional methods, and alkylamino substituents at C5 and C7 installed via Negishi reaction of **41** with 4-cyanobutylzinc bromide (Scheme 7). The disubstituted analogue **43**, however, was found to be weaker (621 nM) than the parent compound.

The most potent analogue **34b** was characterized further in cytokine/chemokine induction profiles in a panel of secondary screens employing human peripheral blood mononuclear cells as well as whole human blood. Consistent with its specificity and potency for TLR8, we observed not only the induction of a specific set of proinflammatory cytokines, including TNF- $\alpha$ , IL-12, and IFN- $\gamma$  (Figure 3), but also that the potency of **34b** was significantly higher than that of both **3** (TLR8-specific) and

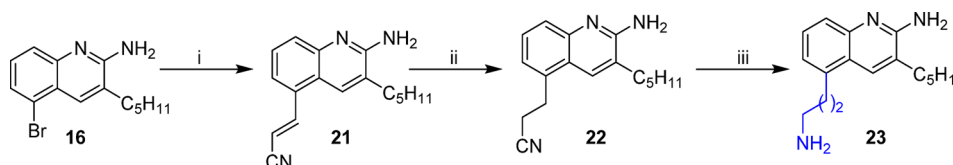
**1** (dual TLR7/8-active). As observed in our previous studies, these agonists also induce responses which are distinctly biphasic, with higher concentrations of ligand leading to an apparent suppression of cytokine production (Figure 3). None of the active compounds displayed any detectable cytotoxicity at concentrations up to 100  $\mu$ g/mL, and the origin of the apparent suppression of responses is presumed to be due to large excesses of ligand disfavoring dimerization of TLR8.

We compared the adjuvantic activity of **34b** (TLR8 EC<sub>50</sub> = 9 nM) with that of **3** (200 nM), as well as a first-generation C2-butylfuro[2,3-*c*]quinoline<sup>57</sup> (1600 nM) in a rabbit model of immunization, using the diphtheria toxin mutein CRM197<sup>72</sup> as a model antigen. CRM197 has served as a carrier protein for conjugate vaccines against encapsulated bacteria such as *Haemophilus influenzae*, *Streptococcus pneumoniae*, and *Neisseria meningitidis*. We observed a clear dependence between antigen-specific IgG titers and TLR8-agonistic potency (Figure 4).

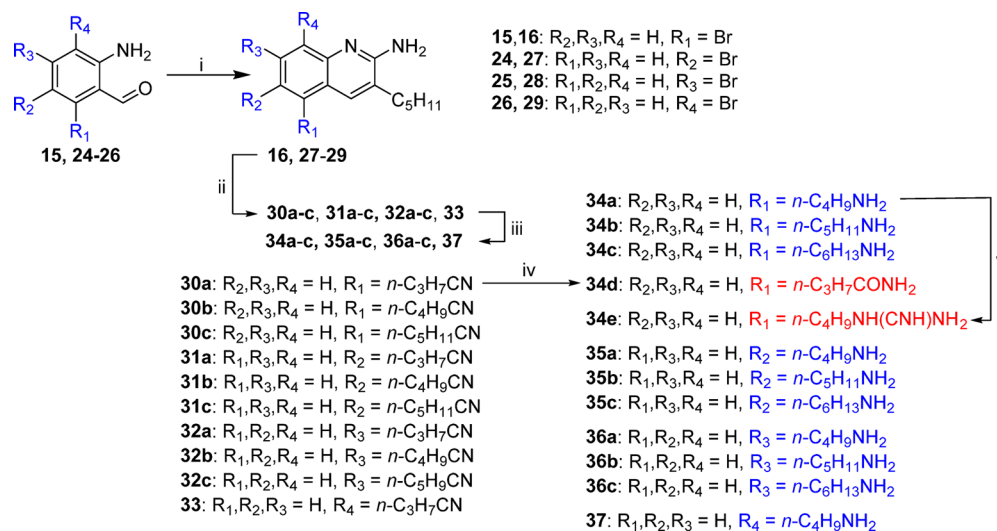
An aspect of our work on vaccine adjuvant discovery, in addition to elucidating of structure–activity relationships in lead candidate vaccine adjuvants, is to delineate specific mechanisms by which these compounds elicit adjuvantic effects. As alluded to earlier, our understanding of how efferent signals arising from activation of the innate immune system engage particular pathways in downstream adaptive immune responses culminating, for instance, in the generation of antigen-specific humoral responses is nascent and fragmentary. One of the questions that we have begun to address is how various chemotypes acting on different innate immune receptors with divergent outcomes effect enhancement of immune responses. Pure TLR8 agonists, as discussed earlier, evoke the production of Th1-biased cytokines such as TNF- $\alpha$ , IL-1, IL-12, IL-18, and IFN- $\gamma$  from cells of the monocytoic lineage; pure TLR7-active compounds induce the copious production of IFN- $\alpha$  from low-abundance plasmacytoid cells, activate natural killer (NK),<sup>73</sup> and induce mitogenicity in B lymphocytes (manuscript in preparation) and are much weaker in inducing TNF- $\alpha$  and IFN- $\gamma$ ; TLR2 agonists, in contrast, activate neutrophils as evidenced by rapid upregulation of CD11b and p38 MAP kinase activity.<sup>43,44</sup> The observation that all these chemotypes display adjuvantic activities may signify that the disparate outcomes in different cell types may point to different mechanisms mediating adjuvantic activities such as, as discussed earlier, enhanced antigen uptake and presentation by APCs,<sup>23–30</sup> enhanced CD4<sup>+</sup> T helper cell activation,<sup>31–33</sup> or affinity maturation of antibodies.<sup>38,39</sup>

In an attempt to understand how TLR8 agonism may modulate adaptive immune functions, we used eight-color flow cytometry to interrogate activation markers (CD40, CD80) in major cellular subsets (granulocytes, monocytes (CD14<sup>+</sup>), T cells (CD3<sup>+</sup>), B cells (CD19<sup>+</sup>), NK cells (CD3<sup>-</sup>CD56<sup>+</sup>), and cytokine-induced killer cells (CD3<sup>+</sup>CD56<sup>+</sup>) in human whole blood stimulated with **34b**, the significantly weaker TLR8-specific **3**,

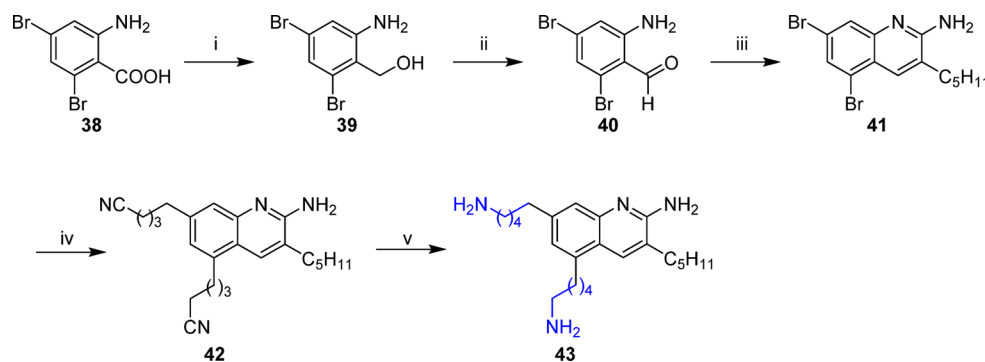
#### Scheme 5<sup>a</sup>



<sup>a</sup>Reagents: (i) acrylonitrile, Pd(OAc)<sub>2</sub>, PPh<sub>3</sub>, K<sub>2</sub>CO<sub>3</sub>, DMF; (ii) H<sub>2</sub>, Pt/C, 30 psi, EtOAc; (iii) LiAlH<sub>4</sub>, THF.

Scheme 6<sup>a</sup>

<sup>a</sup>Reagents: (i) heptanenitrile, *t*-BuOK, DMSO; (ii) 3-cyanopropylzinc bromide (for 30a–32a and 33) or 4-cyanobutylzinc bromide (for 30b–32b) or 5-cyanopentylzinc bromide (for 30c–32c), Pd(PPh<sub>3</sub>)<sub>4</sub>, THF; (iii) LiAlH<sub>4</sub>, THF; (iv) KOH, *t*-BuOH, 8 h; (v) 1*H*-pyrazole-1-carboxamide HCl, Et<sub>3</sub>N, MeOH.

Scheme 7<sup>a</sup>

<sup>a</sup>Reagents: (i) LiAlH<sub>4</sub>, THF; (ii) MnO<sub>2</sub>, DCM; (iii) heptanenitrile, *t*-BuOK, DMSO; (iv) 4-cyanobutylzinc bromide, Pd(PPh<sub>3</sub>)<sub>4</sub>, THF; (v) LiAlH<sub>4</sub>, THF, 4 h.

as well as the potent, dual TLR7/8-active **1**; we found that whereas both **34b** and **1** upregulate CD40, specifically in CD14<sup>+</sup> monocytes (and not in other subsets), the TLR8 stimulation with **34b** strongly induces CD80 expression in the monocytes (Figure 5), and in these assays, differences in potency between **34b** and **1** become readily evident (Figure 5). These results hint at a possible specific role of TLR8 agonists at enhancing antigen presentation and point a way forward to exploring this phenomenon in greater detail.

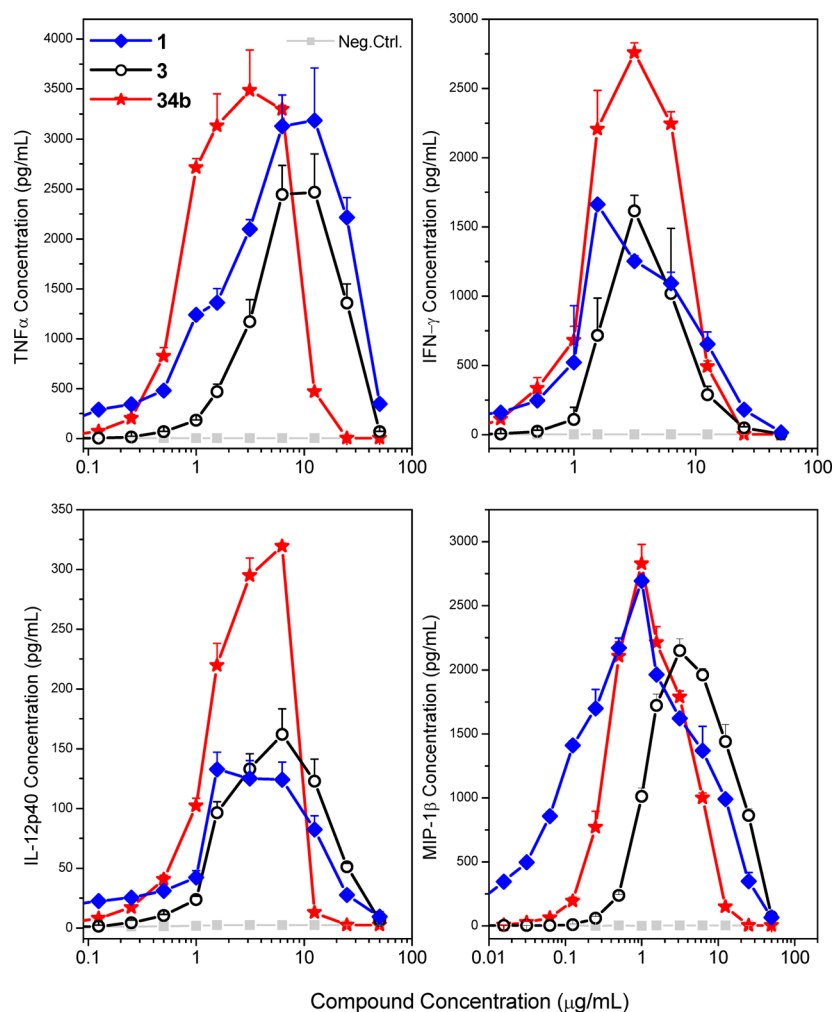
In conclusion, our hypothesis-driven approach of augmenting potency by exploiting key interactions identified in crystallographic studies of TLR8 has yielded novel analogues of extraordinary potency and specificity which are proving useful in understanding the immunological basis of adjuvanticity in this chemotype.

## EXPERIMENTAL SECTION

**Chemistry.** All of the solvents and reagents used were obtained commercially and used as such unless noted otherwise. Moisture- or air-sensitive reactions were conducted under nitrogen atmosphere in oven-dried (120 °C) glass apparatus. Solvents were removed under reduced pressure using standard rotary evaporators. Flash column

chromatography was carried out using RediSep Rf “Gold” high performance silica columns on CombiFlash R<sub>f</sub> instruments unless otherwise mentioned, while thin-layer chromatography was carried out on silica gel CCM precoated aluminum sheets. Purity for all final compounds was confirmed to be greater than 98% by LC–MS using a Zorbax Eclipse Plus 4.6 mm × 150 mm, 5 μm analytical reverse phase C<sub>18</sub> column with H<sub>2</sub>O–CH<sub>3</sub>CN and H<sub>2</sub>O–MeOH gradients and an Agilent 6520 ESI-QTOF accurate mass spectrometer (mass accuracy of 5 ppm) operating in the positive ion acquisition mode. Compound **4** was synthesized as published by us earlier.<sup>58</sup>

**3-((3-(Pent-1-yn-1-yl)quinolin-4-yl)methyl)benzonitrile (5a).** To a solution of compound **4** (230 mg, 1 mmol) in DMF (5 mL) were added 3-cyanobenzylzinc bromide (4 mL, 2 mmol, 0.5 M in THF) and LiCl (85 mg, 2 mmol). The resulting reaction mixture was stirred for 24 h at room temperature under nitrogen atmosphere. The reaction mixture was diluted with water and extracted with EtOAc (3 × 30 mL). The combined organic layer was dried over Na<sub>2</sub>SO<sub>4</sub> and concentrated under reduced pressure. The crude material was purified by flash chromatography (40% EtOAc/hexanes) to obtain the compound **5a** as a pale yellow solid (179 mg, 58%). <sup>1</sup>H NMR (500 MHz, CDCl<sub>3</sub>) δ 8.93 (s, 1H), 8.10 (dd, *J* = 1.2, 8.4 Hz, 1H), 7.87 (dd, *J* = 1.3, 8.3 Hz, 1H), 7.67 (ddd, *J* = 1.3, 6.9, 8.4 Hz, 1H), 7.55–7.50 (m, 2H), 7.49–7.46 (m, 1H), 7.44–7.41 (m, 1H), 7.34 (t, *J* = 7.7 Hz, 1H), 4.65 (s, 2H), 2.47 (t, *J* = 7.0 Hz, 2H), 1.73–1.52 (m, 2H), 1.02



**Figure 3.** Representative cytokine induction data (excerpted from a 63 cytokine panel) in human PBMCs. Mean values  $\pm$  SD on quadruplicates are shown.

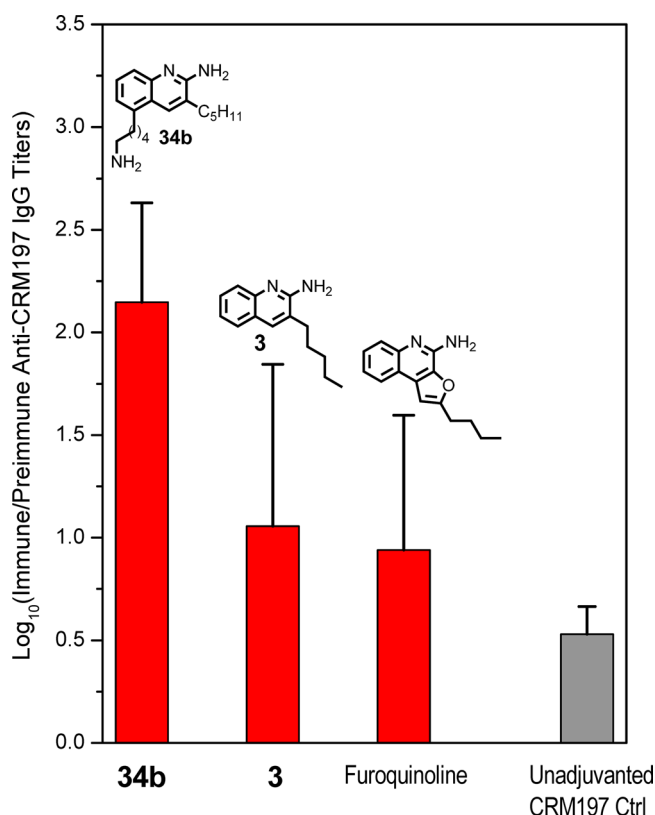
( $t$ ,  $J = 7.4$  Hz, 3H).  $^{13}\text{C}$  NMR (126 MHz,  $\text{CDCl}_3$ )  $\delta$  152.89, 147.08, 145.67, 140.55, 132.90, 132.02, 130.52, 130.36, 129.55, 129.51, 127.65, 126.62, 123.91, 119.01, 118.90, 112.77, 98.31, 77.53, 35.56, 22.20, 21.80, 13.70. MS (ESI-TOF) for  $\text{C}_{22}\text{H}_{18}\text{N}_2$  [ $\text{M} + \text{H}$ ] $^+$  calculated 311.1543, found 311.1441.

**4-((3-(Pent-1-yn-1-yl)quinolin-4-yl)methyl)benzonitrile (5b).** Compound **5b** was synthesized similarly as compound **5a**. 4-Cyano-benzylzinc bromide was used as reagent. Pale yellow solid (201 mg, 65%).  $^1\text{H}$  NMR (500 MHz,  $\text{CDCl}_3$ )  $\delta$  8.93 (s, 1H), 8.09 (dd,  $J = 0.8$ , 8.4 Hz, 1H), 7.84 (dd,  $J = 0.8$ , 8.5 Hz, 1H), 7.67 (ddd,  $J = 1.4$ , 6.9, 8.4 Hz, 1H), 7.56–7.48 (m, 3H), 7.32–7.26 (m, 2H), 4.69 (s, 2H), 2.46 (t,  $J = 7.0$  Hz, 2H), 1.74–1.51 (m, 2H), 1.01 (t,  $J = 7.4$  Hz, 3H).  $^{13}\text{C}$  NMR (126 MHz,  $\text{CDCl}_3$ )  $\delta$  152.87, 147.07, 145.59, 144.64, 132.54, 130.50, 129.55, 129.18, 127.61, 126.68, 123.97, 119.08, 118.94, 110.49, 98.24, 77.50, 36.17, 22.19, 21.79, 13.69. MS (ESI-TOF) for  $\text{C}_{22}\text{H}_{18}\text{N}_2$  [ $\text{M} + \text{H}$ ] $^+$  calculated 311.1543, found 311.1504.

**4-(3-(Aminomethyl)benzyl)-3-pentylquinolin-2-amine Dihydrochloride (9a).** A solution of compound **5a** (155 mg, 0.5 mmol) in THF (5 mL) was added slowly to a solution of  $\text{LiAlH}_4$  (2.5 mL, 2.5 mmol, 1.0 M in THF) in THF (5 mL) at 0  $^\circ\text{C}$  under nitrogen atmosphere. The reaction mixture was stirred for 1 h at 25  $^\circ\text{C}$  and 5 h at 75  $^\circ\text{C}$ . The reaction mixture was cooled to room temperature and quenched carefully with ice-cold water. The resulting mixture was basified with 10% NaOH (to pH = 8.0) and extracted with  $\text{CH}_2\text{Cl}_2$  (3  $\times$  30 mL). The combined organic layer was dried over  $\text{Na}_2\text{SO}_4$  and concentrated under reduced pressure to obtain the residue. The residue was dissolved in MeOH, and di-*tert*-butyl dicarbamate (109 mg, 0.5 mmol) was added and stirred under nitrogen for 1 h. The solvent

was removed under vacuum. The resulting residue was purified by flash chromatography (20% EtOAc/hexanes) to obtain the compound **6a** as a pale yellow solid (134 mg, 65%). MS (ESI-TOF) for  $\text{C}_{27}\text{H}_{30}\text{N}_2\text{O}_2$  [ $\text{M} + \text{H}$ ] $^+$  calculated 415.2380, found 415.2266. To a stirred solution of substrate **6a** (124 mg, 0.3 mmol) in  $\text{CHCl}_3$  was added *m*-CPBA (134 mg, 0.6 mmol). The resulting reaction mixture was stirred for 4 h at room temperature. The reaction mixture was diluted with water and extracted with  $\text{CH}_2\text{Cl}_2$  (3  $\times$  20 mL). The combined organic layer was dried over  $\text{Na}_2\text{SO}_4$ , concentrated under reduced pressure, and the crude material was purified by flash chromatography (10% MeOH/ $\text{CH}_2\text{Cl}_2$ ) to obtain **7a** as a yellow solid (98 mg, 76%). MS (ESI-TOF) for  $\text{C}_{27}\text{H}_{30}\text{N}_2\text{O}_3$  [ $\text{M} + \text{H}$ ] $^+$  calculated 431.2329, found 431.2122. To a stirred solution of **7a** (86 mg, 0.2 mmol) in  $\text{CH}_2\text{Cl}_2$  was added benzoyl isocyanate (88 mg, 0.6 mmol). The resulting reaction mixture was stirred at 55  $^\circ\text{C}$  for 1 h. After completion of reaction (monitored by TLC), the solvent was removed under reduced pressure. The residue was redissolved in MeOH (5 mL), and NaOMe (54 mg, 1 mmol) was added and refluxed for 2 h. The solvent was removed and the crude material was purified by flash chromatography (10% MeOH/ $\text{CH}_2\text{Cl}_2$ ) to obtain **8a** as a off-white solid (67 mg, 78%). MS (ESI-TOF) for  $\text{C}_{27}\text{H}_{31}\text{N}_3\text{O}_2$  [ $\text{M} + \text{H}$ ] $^+$  calculated 430.2489, found 430.2303. To a solution of compound **8a** (43 mg, 0.1 mmol) in anhydrous EtOAc (10 mL) was added a catalytic amount of Pt/C, and the reaction mixture was subjected to hydrogenation at 30 psi for 30 min. The reaction mixture was filtered and the filtrate concentrated under reduced pressure. The crude material was purified by flash chromatography (10% MeOH/ $\text{CH}_2\text{Cl}_2$ ) to obtain *N*-Boc protected benzylamine as a white solid (32 mg). MS (ESI-TOF) for

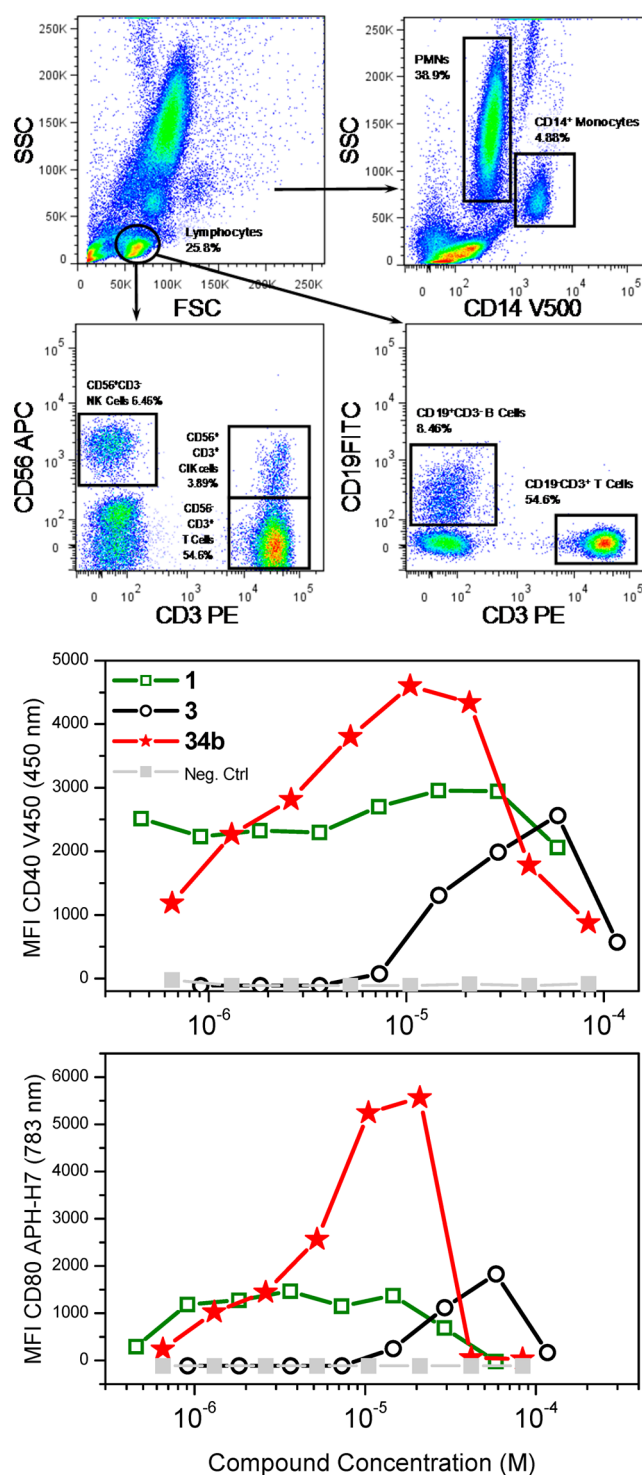




**Figure 4.** Adjuvanticity of TLR8-active compounds. Cohorts of adult female New Zealand white rabbits ( $n = 4$ ) were immunized intramuscularly in the flank region with (a) 10  $\mu\text{g}$  of CRM197 in 0.2 mL of saline (unadjuvanted control) or (b) 10  $\mu\text{g}$  of CRM197 in 0.2 mL of saline plus 100  $\mu\text{g}$  of lead TLR8 agonists (3, 34b, and a TLR8-specific furoquinoline agonist<sup>57</sup>). Preimmune test-bleeds were obtained on day 0, and animals were immunized on days 1, 15, and 28. A final bleed was obtained on day 38. CRM197-specific ELISAs were performed using automated liquid handling methods and are depicted as  $\log_{10}$  (immune/preimmune) titers.

$\text{C}_{27}\text{H}_{35}\text{N}_3\text{O}_2$  [ $\text{M} + \text{H}$ ]<sup>+</sup> calculated 434.2802, found 434.2612. To a stirred solution of *N*-Boc protected benzylamine (32 mg) in 1,4-dioxane (1 mL) was added hydrogen chloride (1 mL, 4 M in dioxane), and the reaction mixture was stirred for 1 h at room temperature. Excess solvent was removed under reduced pressure and the resulting residue was thoroughly washed with diethyl ether to obtain the desired compound 9a as a white solid (28 mg, 69%). <sup>1</sup>H NMR (500 MHz, MeOD)  $\delta$  7.97–7.91 (m, 1H), 7.77–7.64 (m, 2H), 7.43 (ddd,  $J = 1.4, 7.0, 8.4$  Hz, 1H), 7.38 (t,  $J = 7.6$  Hz, 1H), 7.36–7.31 (m, 1H), 7.28 (s, 1H), 7.18 (d,  $J = 8.0$  Hz, 1H), 4.62 (s, 2H), 4.06 (s, 2H), 2.81 (t,  $J = 8.5$  Hz, 2H), 1.58–1.49 (m, 2H), 1.47–1.39 (m, 2H), 1.36–1.25 (m, 2H), 0.89 (t,  $J = 7.3$  Hz, 3H). <sup>13</sup>C NMR (126 MHz, MeOD)  $\delta$  155.07, 151.34, 140.27, 136.23, 135.28, 133.06, 130.87, 129.87, 129.62, 128.43, 127.13, 126.67, 126.32, 123.05, 118.59, 44.08, 34.87, 32.75, 29.22, 28.11, 23.67, 14.34. MS (ESI-TOF) for  $\text{C}_{22}\text{H}_{27}\text{N}_3$  [ $\text{M} + \text{H}$ ]<sup>+</sup> calculated 334.2278, found 334.2238.

**4-(4-(Aminomethyl)benzyl)-3-pentylquinolin-2-amine Dihydrochloride (9b).** Compound 9b was synthesized similarly as compound 9a. White solid (30 mg, 74%). <sup>1</sup>H NMR (500 MHz, MeOD)  $\delta$  7.91 (dd,  $J = 1.2, 8.4$  Hz, 1H), 7.79–7.64 (m, 2H), 7.44–7.37 (m, 3H), 7.22 (d,  $J = 8.0$  Hz, 2H), 4.62 (s, 2H), 4.07 (s, 2H), 2.79 (t,  $J = 8.2$  Hz, 2H), 1.57–1.47 (m, 2H), 1.46–1.38 (m, 2H), 1.36–1.27 (m, 2H), 0.89 (t,  $J = 7.3$  Hz, 3H). <sup>13</sup>C NMR (126 MHz, MeOD)  $\delta$  155.04, 151.56, 140.37, 136.15, 133.09, 133.07, 130.67, 129.85, 127.14, 126.60, 126.20, 123.00, 118.56, 43.87, 34.72, 32.71, 29.19, 27.99, 23.62, 14.33. MS (ESI-TOF) for  $\text{C}_{22}\text{H}_{27}\text{N}_3$  [ $\text{M} + \text{H}$ ]<sup>+</sup> calculated 334.2278, found 334.2257.



**Figure 5.** Eight-color flow cytometry. Top: gating strategy for identification of B, T, NK lymphocytes, monocytes, and granulocytes. Monocytes were identified directly based on CD14<sup>+</sup> phenotype. Lymphocytic subsets were identified based on CD3, CD19, CD56 staining patterns as described in the [Experimental Section](#). Bottom: stimulation of whole human blood TLR8-active compounds leading to upregulation of CD40 and CD80 in CD14<sup>+</sup> monocytes, denoted by increase in mean fluorescence intensity (MFI).

**4-(3-(Pent-1-yn-1-yl)quinolin-4-yl)butanenitrile (10a).** To a solution of compound 4 (229.7 mg, 1 mmol) in THF (4 mL) were added 3-cyanopropylzinc bromide (4 mL, 2 mmol, 0.5 M in THF) and Pd(PPh<sub>3</sub>)<sub>4</sub> (115.5 mg, 0.1 mmol). The resulting reaction mixture was

stirred for 12 h at 65 °C under nitrogen atmosphere. The reaction mixture was diluted with water and extracted with EtOAc (3 × 30 mL). The combined organic layer was dried over Na<sub>2</sub>SO<sub>4</sub> and concentrated under reduced pressure. The crude material was purified by flash chromatography (20% EtOAc/hexanes) to obtain the compound **10a** as a pale yellow oil (144 mg, 55%). <sup>1</sup>H NMR (500 MHz, CDCl<sub>3</sub>) δ 8.84 (s, 1H), 8.11–8.06 (m, 1H), 7.98 (dd, *J* = 1.0, 8.9 Hz, 1H), 7.69 (ddd, *J* = 1.3, 6.8, 8.3 Hz, 1H), 7.59 (ddd, *J* = 1.3, 6.8, 8.3 Hz, 1H), 3.42 (t, *J* = 7.7 Hz, 2H), 2.53 (t, *J* = 7.0 Hz, 2H), 2.46 (t, *J* = 7.0 Hz, 2H), 2.14–2.03 (m, 2H), 1.77–1.62 (m, 2H), 1.10 (t, *J* = 7.4 Hz, 3H). <sup>13</sup>C NMR (126 MHz, CDCl<sub>3</sub>) δ 152.74, 147.14, 146.93, 130.56, 129.49, 127.51, 126.37, 123.25, 119.48, 118.15, 98.32, 77.10, 28.90, 25.79, 22.27, 21.83, 17.31, 13.81. MS (ESI-TOF) for C<sub>18</sub>H<sub>18</sub>N<sub>2</sub> [M + H]<sup>+</sup> calculated 263.1543, found 263.1437.

**5-(3-(Pent-1-yn-1-yl)quinolin-4-yl)pentanenitrile (10b).** Compound **10b** was synthesized similarly as compound **10a**. 4-Cyano-butylzinc bromide was used as reagent. Pale yellow oil (174 mg, 63%). <sup>1</sup>H NMR (500 MHz, CDCl<sub>3</sub>) δ 8.83 (s, 1H), 8.07 (dd, *J* = 0.8, 8.5 Hz, 1H), 7.97 (dd, *J* = 1.0, 8.5 Hz, 1H), 7.67 (ddd, *J* = 1.4, 6.9, 8.3 Hz, 1H), 7.57 (ddd, *J* = 1.3, 6.9, 8.3 Hz, 1H), 3.30 (t, *J* = 7.5 Hz, 2H), 2.51 (t, *J* = 7.0 Hz, 2H), 2.40 (t, *J* = 7.0 Hz, 2H), 1.95–1.84 (m, 2H), 1.85–1.75 (m, 2H), 1.76–1.65 (m, 2H), 1.10 (t, *J* = 7.4 Hz, 3H). <sup>13</sup>C NMR (126 MHz, CDCl<sub>3</sub>) δ 152.78, 148.54, 146.91, 130.45, 129.34, 127.22, 126.48, 123.54, 119.52, 117.88, 97.62, 77.51, 29.32, 29.02, 25.41, 22.33, 21.81, 17.20, 13.79. MS (ESI-TOF) for C<sub>19</sub>H<sub>20</sub>N<sub>2</sub> [M + H]<sup>+</sup> calculated 277.1699, found 277.1581.

**4-(4-Aminobutyl)-3-pentylquinolin-2-amine Dihydrochloride (14a).** Compound **14a** was synthesized similarly as compound **9a**. White solid (28 mg, 78%). <sup>1</sup>H NMR (500 MHz, MeOD) δ 8.11 (d, *J* = 8.1 Hz, 1H), 7.76 (ddd, *J* = 1.2, 7.1, 8.4 Hz, 1H), 7.67 (dd, *J* = 1.2, 8.4 Hz, 1H), 7.57 (ddd, *J* = 1.2, 7.1, 8.3 Hz, 1H), 3.19 (t, *J* = 8.2 Hz, 2H), 3.01 (t, *J* = 7.6 Hz, 2H), 2.80 (t, *J* = 8.2 Hz, 2H), 1.98–1.87 (m, 2H), 1.80–1.70 (m, 2H), 1.65–1.55 (m, 2H), 1.56–1.46 (m, 2H), 1.47–1.38 (m, 2H), 0.96 (t, *J* = 7.2 Hz, 3H). <sup>13</sup>C NMR (126 MHz, MeOD) δ 154.80, 154.01, 135.98, 133.05, 126.77, 126.45, 124.51, 122.47, 118.61, 40.50, 32.81, 29.52, 29.45, 28.86, 28.16, 27.56, 23.73, 14.42. MS (ESI-TOF) for C<sub>18</sub>H<sub>27</sub>N<sub>3</sub> [M + H]<sup>+</sup> calculated 286.2278, found 286.2240.

**4-(5-Aminopentyl)-3-pentylquinolin-2-amine Dihydrochloride (14b).** Compound **14b** was synthesized similarly as compound **9a**. White solid (29 mg, 78%). <sup>1</sup>H NMR (500 MHz, MeOD) δ 8.09 (d, *J* = 8.2 Hz, 1H), 7.76 (ddd, *J* = 1.2, 7.0, 8.3 Hz, 1H), 7.66 (d, *J* = 7.6 Hz, 1H), 7.56 (ddd, *J* = 1.2, 7.0, 8.3 Hz, 1H), 3.16 (t, *J* = 6.7 Hz, 2H), 2.97 (t, *J* = 7.5 Hz, 2H), 2.79 (t, *J* = 8.4 Hz, 2H), 1.80–1.64 (m, 6H), 1.64–1.56 (m, 2H), 1.54–1.46 (m, 2H), 1.48–1.38 (m, 2H), 0.96 (t, *J* = 7.3 Hz, 3H). <sup>13</sup>C NMR (126 MHz, MeOD) δ 154.78, 154.54, 135.97, 133.00, 126.70, 126.41, 124.30, 122.51, 118.60, 40.61, 32.81, 30.92, 29.79, 29.52, 28.48, 27.85, 27.54, 23.73, 14.41. MS (ESI-TOF) for C<sub>19</sub>H<sub>29</sub>N<sub>3</sub> [M + H]<sup>+</sup> calculated 300.2434, found 300.2397.

**5-Bromo-3-pentylquinolin-2-amine (16).** To a solution of compound **15** (200 mg, 1 mmol) in DMSO (3 mL) were added heptanenitrile (275 μL, 2 mmol) and *t*-BuOK (224 mg, 2 mmol). The resulting reaction mixture was stirred for 3 h at 60 °C under nitrogen atmosphere. The reaction mixture was diluted with water and extracted with EtOAc (3 × 50 mL). The combined organic layer was dried over Na<sub>2</sub>SO<sub>4</sub> and concentrated under reduced pressure. The crude material was purified by flash chromatography (50% EtOAc/hexanes) to obtain the compound **16** as an off-white solid (220 mg, 75%). <sup>1</sup>H NMR (500 MHz, DMSO-*d*<sub>6</sub>) δ 7.82 (s, 1H), 7.49–7.40 (m, 2H), 7.34 (dd, *J* = 7.6, 8.3 Hz, 1H), 6.58 (s, 2H), 2.62 (t, *J* = 7.8 Hz, 2H), 1.66–1.57 (m, 2H), 1.44–1.29 (m, 4H), 0.89 (t, *J* = 7.0 Hz, 3H). <sup>13</sup>C NMR (126 MHz, DMSO-*d*<sub>6</sub>) δ 157.75, 147.59, 132.61, 128.85, 126.08, 124.89, 124.73, 121.98, 120.40, 30.96, 30.29, 27.42, 22.06, 14.01. MS (ESI-TOF) for C<sub>14</sub>H<sub>17</sub>BrN<sub>2</sub> [M + H]<sup>+</sup> calculated 293.0648, found 293.0684.

**3-((2-Amino-3-pentylquinolin-5-yl)methyl)benzonitrile (17a).** To a solution of compound **16** (58.8 mg, 0.2 mmol) in THF (2 mL) were added 3-cyanobenzylzinc bromide (0.8 mL, 0.4 mmol, 0.5 M in THF) and Pd(PPh<sub>3</sub>)<sub>4</sub> (11.6 mg, 0.01 mmol). The resulting reaction mixture was stirred at 65 °C under nitrogen atmosphere for

12 h. The reaction mixture was diluted with water and extracted with EtOAc (3 × 10 mL). The combined organic layer was dried over Na<sub>2</sub>SO<sub>4</sub> and concentrated under reduced pressure. The crude material was purified by flash chromatography (60% EtOAc/hexanes) to obtain the compound **17a** as a pale yellow solid (54 mg, 82%). <sup>1</sup>H NMR (500 MHz, CDCl<sub>3</sub>) δ 7.67 (s, 1H), 7.61 (d, *J* = 8.5 Hz, 1H), 7.51–7.44 (m, 3H), 7.40–7.33 (m, 2H), 7.07 (d, *J* = 7.0 Hz, 1H), 4.80 (s, 2H), 4.37 (s, 2H), 2.52 (t, *J* = 7.6 Hz, 2H), 1.66–1.56 (m, 2H), 1.38–1.21 (m, 4H), 0.88 (t, *J* = 7.1 Hz, 3H). <sup>13</sup>C NMR (126 MHz, CDCl<sub>3</sub>) δ 155.95, 147.28, 142.44, 134.55, 133.17, 132.16, 131.77, 130.13, 129.40, 128.69, 125.59, 124.49, 123.66, 122.91, 119.00, 112.68, 38.40, 31.52, 31.49, 27.56, 22.63, 14.15. MS (ESI-TOF) for C<sub>22</sub>H<sub>23</sub>N<sub>3</sub> [M + H]<sup>+</sup> calculated 330.1965, found 330.1896.

**Compounds 17b–d.** They were synthesized similarly as compound **17a**.

**4-((2-Amino-3-pentylquinolin-5-yl)methyl)benzonitrile (17b).** 4-Cyanobenzylzinc bromide was used as reagent. Pale yellow solid (55 mg, 83%). <sup>1</sup>H NMR (500 MHz, CDCl<sub>3</sub>) δ 7.66 (s, 1H), 7.62 (d, *J* = 8.5 Hz, 1H), 7.56 (d, *J* = 8.3 Hz, 2H), 7.48 (dd, *J* = 7.0, 8.4 Hz, 1H), 7.30–7.25 (m, 2H), 7.09 (d, *J* = 6.8 Hz, 1H), 4.81 (s, 2H), 4.41 (s, 2H), 2.52 (t, *J* = 7.8 Hz, 2H), 1.66–1.53 (m, 2H), 1.39–1.19 (m, 4H), 0.89 (t, *J* = 7.1 Hz, 3H). <sup>13</sup>C NMR (126 MHz, CDCl<sub>3</sub>) δ 155.95, 147.26, 146.62, 134.50, 132.44, 131.82, 129.42, 128.68, 125.56, 124.54, 123.63, 122.96, 119.07, 110.20, 39.00, 31.51, 31.45, 27.53, 22.63, 14.15. MS (ESI-TOF) for C<sub>22</sub>H<sub>23</sub>N<sub>3</sub> [M + H]<sup>+</sup> calculated 330.1965, found 330.1899.

**2-((2-Amino-3-pentylquinolin-5-yl)methyl)benzonitrile (17c).** 2-Cyanobenzylzinc bromide was used as reagent. Pale yellow solid (45 mg, 68%). <sup>1</sup>H NMR (500 MHz, CDCl<sub>3</sub>) δ 7.71 (s, 1H), 7.69 (dd, *J* = 1.1, 7.7 Hz, 1H), 7.61 (d, *J* = 8.5 Hz, 1H), 7.47 (dd, *J* = 7.1, 8.5 Hz, 1H), 7.39 (td, *J* = 1.4, 7.7 Hz, 1H), 7.29 (td, *J* = 1.2, 7.6 Hz, 1H), 7.07 (dd, *J* = 1.1, 7.1 Hz, 1H), 7.00 (dd, *J* = 0.6, 7.9 Hz, 1H), 4.81 (s, 2H), 4.57 (s, 2H), 2.53 (t, *J* = 7.6 Hz, 2H), 1.67–1.60 (m, 2H), 1.38–1.22 (m, 4H), 0.87 (t, *J* = 7.1 Hz, 3H). <sup>13</sup>C NMR (126 MHz, CDCl<sub>3</sub>) δ 156.01, 147.18, 144.65, 134.08, 133.05, 132.87, 131.83, 129.79, 128.64, 126.92, 125.57, 124.59, 123.80, 123.06, 118.25, 112.43, 36.89, 31.56, 31.48, 27.55, 22.62, 14.16. MS (ESI-TOF) for C<sub>22</sub>H<sub>23</sub>N<sub>3</sub> [M + H]<sup>+</sup> calculated 330.1965, found 330.2008.

**5-Benzyl-3-pentylquinolin-2-amine (17d).** Benzylzinc bromide was used as reagent. White solid (50 mg, 82%). <sup>1</sup>H NMR (500 MHz, DMSO-*d*<sub>6</sub>) δ 7.82 (s, 1H), 7.41–7.31 (m, 2H), 7.28–7.18 (m, 4H), 7.18–7.11 (m, 1H), 7.05–7.00 (m, 1H), 6.21 (s, 2H), 4.28 (s, 2H), 2.55–2.49 (m, 2H), 1.57–1.47 (m, 2H), 1.32–1.17 (m, 4H), 0.83 (t, *J* = 7.2 Hz, 3H). <sup>13</sup>C NMR (126 MHz, DMSO-*d*<sub>6</sub>) δ 156.73, 147.10, 141.09, 136.57, 131.20, 128.43, 128.28, 127.75, 125.84, 123.78, 123.50, 122.48, 121.73, 37.77, 30.72, 30.31, 27.23, 22.06, 13.96. MS (ESI-TOF) for C<sub>21</sub>H<sub>24</sub>N<sub>2</sub> [M + H]<sup>+</sup> calculated 305.2012, found 305.1951.

**5-(3-(Aminomethyl)benzyl)-3-pentylquinolin-2-amine (18a).** A solution of compound **17a** (33 mg, 0.1 mmol) in THF (5 mL) was added slowly to a solution of LiAlH<sub>4</sub> (0.5 mL, 0.5 mmol, 1.0 M in THF) in THF (3 mL) at 0 °C under nitrogen atmosphere. The reaction mixture was stirred for 2 h at 25 °C and 2 h at 75 °C. The reaction mixture was carefully quenched with ice-cold water (1 mL) at 0 °C, and 10% NaOH (1 mL) was added. The resulting mixture was stirred for 10 min at room temperature, filtered through Celite, and washed with CH<sub>2</sub>Cl<sub>2</sub> (15 mL). The resulting filtrate was dried over Na<sub>2</sub>SO<sub>4</sub> and concentrated under reduced pressure and the crude material was purified by neutral-alumina column chromatography (20% MeOH/CH<sub>2</sub>Cl<sub>2</sub>) to obtain the compound **18a** as a white solid (24 mg, 72%). <sup>1</sup>H NMR (500 MHz, MeOD) δ 7.88 (s, 1H), 7.46–7.38 (m, 2H), 7.21 (t, *J* = 7.5 Hz, 1H), 7.18–7.10 (m, 3H), 7.06 (d, *J* = 7.4 Hz, 1H), 4.34 (s, 2H), 3.70 (s, 2H), 2.55 (t, *J* = 7.5 Hz, 2H), 1.60 (p, *J* = 7.6 Hz, 2H), 1.42–1.20 (m, 4H), 0.89 (t, *J* = 7.1 Hz, 3H). <sup>13</sup>C NMR (126 MHz, MeOD) δ 158.00, 147.60, 143.84, 142.65, 138.04, 133.82, 129.68, 129.58, 128.69, 128.24, 126.21, 125.12, 125.06, 124.29, 123.67, 46.67, 39.64, 32.47, 31.77, 28.68, 23.64, 14.41. MS (ESI-TOF) for C<sub>22</sub>H<sub>27</sub>N<sub>3</sub> [M + H]<sup>+</sup> calculated 334.2278, found 334.2214.

**Compounds 18b and 18c.** They were synthesized similarly as compound **18a**.

**5-(4-(Aminomethyl)benzyl)-3-pentylquinolin-2-amine (18b).**

Compound 17b was used as reagent. White solid (25 mg, 75%). <sup>1</sup>H NMR (500 MHz, MeOD) δ 7.87 (s, 1H), 7.51–7.37 (m, 2H), 7.22 (d, *J* = 8.0 Hz, 2H), 7.14 (d, *J* = 7.9 Hz, 2H), 7.12–7.09 (m, 1H), 4.32 (s, 2H), 3.72 (s, 2H), 2.54 (t, *J* = 7.6 Hz, 2H), 1.68–1.48 (m, 2H), 1.40–1.21 (m, 4H), 0.89 (t, *J* = 7.1 Hz, 3H). <sup>13</sup>C NMR (126 MHz, MeOD) δ 158.00, 147.60, 141.33, 141.04, 138.13, 133.81, 129.74, 129.56, 128.59, 125.10, 124.98, 124.27, 123.63, 46.35, 39.28, 32.48, 31.78, 28.66, 23.64, 14.41. MS (ESI-TOF) for C<sub>22</sub>H<sub>27</sub>N<sub>3</sub> [M + H]<sup>+</sup> calculated 334.2278, found 334.2191.

**5-(2-(Aminomethyl)benzyl)-3-pentylquinolin-2-amine (18c).**

Compound 17c was used as reagent. White solid (21 mg, 63%). <sup>1</sup>H NMR (500 MHz, MeOD) δ 7.90 (s, 1H), 7.47–7.33 (m, 3H), 7.24 (td, *J* = 1.3, 7.5 Hz, 1H), 7.15 (td, *J* = 1.4, 7.5 Hz, 1H), 6.93 (dd, *J* = 1.3, 7.7 Hz, 1H), 6.84 (dd, *J* = 1.1, 7.1 Hz, 1H), 4.42 (s, 2H), 3.84 (s, 2H), 2.59 (t, *J* = 7.8 Hz, 2H), 1.68–1.57 (m, 2H), 1.40–1.27 (m, 4H), 0.90 (t, *J* = 7.1 Hz, 3H). <sup>13</sup>C NMR (126 MHz, MeOD) δ 158.12, 147.46, 141.29, 139.25, 137.80, 133.50, 131.09, 129.58, 129.13, 128.27, 127.89, 125.42, 124.27, 124.19, 123.78, 43.84, 35.93, 32.58, 31.94, 28.87, 23.65, 14.42. MS (ESI-TOF) for C<sub>22</sub>H<sub>27</sub>N<sub>3</sub> [M + H]<sup>+</sup> calculated 334.2278, found 334.2195.

**3-((2-Amino-3-pentylquinolin-5-yl)methyl)benzamide (18d).**

To a solution of compound 17a (33 mg, 0.1 mmol) in *t*-BuOH (2 mL) was added potassium hydroxide (84 mg, 1.5 mmol). The reaction mixture was stirred for 8 h at 60 °C. The reaction was allowed to cool to room temperature, the solvent was removed under reduced pressure and the crude solubilized in ethyl acetate. The organic layer was washed with water and saturated aqueous ammonium chloride and dried over Na<sub>2</sub>SO<sub>4</sub> and evaporated under reduced pressure. The residue was purified by silica gel flash-column chromatography (15% MeOH/CH<sub>2</sub>Cl<sub>2</sub>) to afford the compound (18d) as a white solid (18 mg, 52%). <sup>1</sup>H NMR (500 MHz, MeOD) δ 7.88 (s, 1H), 7.78 (d, *J* = 0.8 Hz, 1H), 7.68 (dt, *J* = 1.9, 7.0 Hz, 1H), 7.49–7.43 (m, 2H), 7.38–7.27 (m, 2H), 7.16 (dd, *J* = 3.2, 5.0 Hz, 1H), 4.42 (s, 2H), 2.56 (t, *J* = 7.1 Hz, 2H), 1.58 (p, *J* = 7.5 Hz, 2H), 1.36–1.27 (m, 2H), 1.28–1.19 (m, 2H), 0.86 (t, *J* = 7.2 Hz, 3H). <sup>13</sup>C NMR (126 MHz, MeOD) δ 172.26, 157.87, 147.04, 142.96, 137.61, 135.13, 134.03, 133.11, 129.84, 129.66, 128.98, 126.42, 125.39, 125.32, 124.08, 123.44, 39.47, 32.39, 31.68, 28.61, 23.59, 14.39. MS (ESI-TOF) for C<sub>22</sub>H<sub>25</sub>N<sub>3</sub>O [M + H]<sup>+</sup> calculated 348.2070, found 348.2022.

**3-(2-Amino-3-pentylquinolin-5-yl)benzonitrile (19a).**

To a stirred solution of compound 16 (59 mg, 0.2 mmol) in 1,4-dioxane (2 mL) were added 3-cyanophenylboronic acid (44 mg, 0.3 mmol), Pd(dppf)Cl<sub>2</sub> (14.6 mg, 0.02 mmol), and K<sub>2</sub>CO<sub>3</sub> (83 mg, 0.6 mmol). The resulting reaction mixture was stirred for 12 h at 90 °C under nitrogen atmosphere. The reaction mixture was diluted with water and extracted with EtOAc (3 × 20 mL). The combined organic layer was dried over Na<sub>2</sub>SO<sub>4</sub> and concentrated under reduced pressure, and crude material was purified by flash chromatography (60% EtOAc/hexanes) to obtain the compound 19a as a brownish solid (40 mg, 63%). <sup>1</sup>H NMR (500 MHz, CDCl<sub>3</sub>) δ 7.77–7.66 (m, 4H), 7.64–7.52 (m, 3H), 7.15 (dd, *J* = 1.2, 7.1 Hz, 1H), 4.89 (s, 2H), 2.53 (t, *J* = 7.6 Hz, 2H), 1.67–1.57 (m, 2H), 1.39–1.31 (m, 4H), 0.89 (t, *J* = 6.9 Hz, 3H). <sup>13</sup>C NMR (126 MHz, CDCl<sub>3</sub>) δ 156.25, 146.96, 141.74, 137.22, 134.46, 133.42, 132.79, 131.10, 129.35, 128.42, 126.31, 124.37, 123.92, 122.25, 118.90, 112.78, 31.69, 31.59, 27.74, 22.57, 14.15. MS (ESI-TOF) for C<sub>21</sub>H<sub>21</sub>N<sub>3</sub> [M + H]<sup>+</sup> calculated 316.1808, found 316.1823.

**4-(2-Amino-3-pentylquinolin-5-yl)benzonitrile (19b).**

Compound 19b was synthesized similarly as compound 19a. 4-Cyanophenylboronic acid was used as reagent. Brownish solid (38 mg, 60%). <sup>1</sup>H NMR (500 MHz, CDCl<sub>3</sub>) δ 7.83–7.76 (m, 2H), 7.71 (d, *J* = 8.4 Hz, 1H), 7.61 (s, 1H), 7.60–7.53 (m, 3H), 7.17 (dd, *J* = 1.2, 7.2 Hz, 1H), 4.89 (s, 2H), 2.52 (t, *J* = 7.7 Hz, 2H), 1.67–1.55 (m, 2H), 1.40–1.31 (m, 4H), 0.89 (t, *J* = 7.0 Hz, 3H). <sup>13</sup>C NMR (126 MHz, CDCl<sub>3</sub>) δ 156.24, 146.97, 145.32, 137.73, 132.84, 132.32, 130.78, 128.40, 126.40, 124.35, 123.80, 122.09, 119.04, 111.30, 31.68, 31.56, 27.73, 22.57, 14.16. MS (ESI-TOF) for C<sub>21</sub>H<sub>21</sub>N<sub>3</sub> [M + H]<sup>+</sup> calculated 316.1808, found 316.1845.

**Compounds 20a,b**. They were synthesized similarly as compound 18a.

**5-(3-(Aminomethyl)phenyl)-3-pentylquinolin-2-amine (20a).**

Compound 19a was used as reagent. White solid (21 mg, 66%). <sup>1</sup>H NMR (500 MHz, MeOD) δ 7.73 (s, 1H), 7.58–7.39 (m, 5H), 7.30 (d, *J* = 6.7 Hz, 1H), 7.16 (d, *J* = 6.6 Hz, 1H), 3.88 (s, 2H), 2.56 (t, *J* = 7.6 Hz, 2H), 1.68–1.53 (m, 2H), 1.38–1.29 (m, 4H), 0.90 (t, *J* = 6.7 Hz, 3H). <sup>13</sup>C NMR (126 MHz, MeOD) δ 158.28, 147.40, 144.04, 141.73, 141.28, 134.86, 130.00, 129.55, 129.53, 129.41, 127.59, 125.60, 124.69, 124.34, 123.07, 46.69, 32.56, 31.81, 28.73, 23.59, 14.39. MS (ESI-TOF) for C<sub>21</sub>H<sub>25</sub>N<sub>3</sub> [M + H]<sup>+</sup> calculated 320.2121, found 320.2072.

**5-(4-(Aminomethyl)phenyl)-3-pentylquinolin-2-amine (20b).**

Compound 19b was used as reagent. White solid (20 mg, 63%). <sup>1</sup>H NMR (500 MHz, MeOD) δ 7.72 (s, 1H), 7.57–7.45 (m, 4H), 7.39 (d, *J* = 8.1 Hz, 2H), 7.13 (dd, *J* = 1.7, 6.6 Hz, 1H), 3.89 (s, 2H), 2.54 (t, *J* = 7.6 Hz, 2H), 1.67–1.51 (m, 2H), 1.38–1.26 (m, 4H), 0.89 (t, *J* = 7.0 Hz, 3H). <sup>13</sup>C NMR (126 MHz, MeOD) δ 158.26, 147.42, 142.97, 141.07, 140.07, 134.82, 131.06, 129.43, 128.56, 125.58, 124.65, 124.33, 123.07, 46.45, 32.58, 31.88, 28.78, 23.57, 14.40. MS (ESI-TOF) for C<sub>21</sub>H<sub>25</sub>N<sub>3</sub> [M + H]<sup>+</sup> calculated 320.2121, found 320.2073.

**5-(3-Aminopropyl)-3-pentylquinolin-2-amine (23).**

A solution of 16 (147 mg, 0.5 mmol) and acrylonitrile (66 μL, 1 mmol) in DMF (4 mL) was treated with Pd(OAc)<sub>2</sub> (11.2 mg, 0.05 mmol), PPh<sub>3</sub> (26.2 mg, 0.1 mmol), and K<sub>2</sub>CO<sub>3</sub> (138 mg, 1 mmol). The resulting reaction mixture was stirred for 12 h at 110 °C under nitrogen atmosphere. The reaction mixture was diluted with water and extracted with EtOAc (3 × 20 mL). The combined organic layer was dried over Na<sub>2</sub>SO<sub>4</sub> and concentrated under reduced pressure. The crude material was purified by flash chromatography (60% EtOAc/hexanes) to obtain the compound 21 as a pale yellow solid (73 mg, 55%). MS (ESI-TOF) for C<sub>17</sub>H<sub>19</sub>N<sub>3</sub> [M + H]<sup>+</sup> calculated 266.1652, found 266.1663. To a solution of compound 21 (53 mg, 0.2 mmol) in anhydrous EtOAc (10 mL) was added a catalytic amount of Pt/C, and the reaction mixture was subjected to hydrogenation at 30 psi for 3 h. The reaction mixture was filtered, and the filtrate concentrated under reduced pressure. The crude material was purified using silica gel column chromatography (60% EtOAc/hexanes) to obtain compound 22 as white solid (40 mg, 75%). MS (ESI-TOF) for C<sub>17</sub>H<sub>21</sub>N<sub>3</sub> [M + H]<sup>+</sup> calculated 268.1808, found 268.1821. A solution of compound 22 (27 mg, 0.1 mmol) in THF (5 mL) was added slowly to a solution of LiAlH<sub>4</sub> (0.5 mL, 0.5 mmol, 1.0 M in THF) in THF (3 mL) at 0 °C under nitrogen atmosphere. The reaction mixture was stirred for 2 h at 25 °C and 2 h at 60 °C. The reaction mixture was carefully quenched with ice-cold water (1 mL) at 0 °C, and 10% NaOH (1 mL) was added. The resulting mixture was stirred for 10 min at room temperature, filtered through Celite, and washed with CH<sub>2</sub>Cl<sub>2</sub> (15 mL). The resulting filtrate was dried over Na<sub>2</sub>SO<sub>4</sub> and concentrated under reduced pressure and the crude material was purified by flash neutral-alumina column chromatography (20% MeOH/CH<sub>2</sub>Cl<sub>2</sub>) to obtain the compound 23 as a white solid (15 mg, 55%). <sup>1</sup>H NMR (500 MHz, MeOD) δ 7.99 (s, 1H), 7.40–7.37 (m, 2H), 7.09 (dd, *J* = 2.8, 5.4 Hz, 1H), 3.02 (t, *J* = 7.5 Hz, 2H), 2.73 (t, *J* = 7.2 Hz, 2H), 2.68 (t, *J* = 7.6 Hz, 2H), 1.92–1.80 (m, 2H), 1.78–1.68 (m, 2H), 1.48–1.40 (m, 4H), 0.95 (t, *J* = 7.1 Hz, 3H). <sup>13</sup>C NMR (126 MHz, MeOD) δ 158.00, 147.49, 139.44, 133.35, 129.58, 125.36, 123.72, 123.66, 123.41, 42.35, 35.26, 32.80, 32.15, 30.76, 29.17, 23.69, 14.46. MS (ESI-TOF) for C<sub>17</sub>H<sub>25</sub>N<sub>3</sub> [M + H]<sup>+</sup> calculated 272.2121, found 272.2155.

**Compounds 27–29.** They were synthesized similarly as compound 16.

**6-Bromo-3-pentylquinolin-2-amine (27).**

Compound 24 was used as reagent. White solid (230 mg, 78%). <sup>1</sup>H NMR (500 MHz, CDCl<sub>3</sub>) δ 7.74 (d, *J* = 2.2 Hz, 1H), 7.58 (s, 1H), 7.56 (dd, *J* = 2.2, 8.9 Hz, 1H), 7.51 (d, *J* = 8.8 Hz, 1H), 4.87 (s, 2H), 2.57 (t, *J* = 7.7 Hz, 2H), 1.78–1.66 (m, 2H), 1.45–1.36 (m, 4H), 0.93 (t, *J* = 7.0 Hz, 3H). <sup>13</sup>C NMR (126 MHz, CDCl<sub>3</sub>) δ 156.49, 145.21, 134.44, 132.05, 129.08, 127.43, 125.84, 124.79, 115.57, 31.76, 31.24, 27.56, 22.67, 14.17. MS (ESI-TOF) for C<sub>14</sub>H<sub>17</sub>BrN<sub>2</sub> [M + H]<sup>+</sup> calculated 293.0648, found 293.0654.

**7-Bromo-3-pentylquinolin-2-amine (28).** Compound **25** was used as reagent. Yellow solid (220 mg, 75%).  $^1\text{H}$  NMR (500 MHz,  $\text{CDCl}_3$ )  $\delta$  7.81 (d,  $J = 2.2$  Hz, 1H), 7.63 (s, 1H), 7.45 (d,  $J = 8.5$  Hz, 1H), 7.32 (dd,  $J = 1.9, 8.5$  Hz, 1H), 4.93 (s, 2H), 2.55 (t,  $J = 7.9$  Hz, 2H), 1.76–1.67 (m, 2H), 1.44–1.36 (m, 4H), 0.93 (t,  $J = 7.0$  Hz, 3H).  $^{13}\text{C}$  NMR (126 MHz,  $\text{CDCl}_3$ )  $\delta$  156.88, 147.41, 135.17, 128.30, 128.09, 125.98, 124.16, 123.19, 122.73, 31.79, 31.24, 27.56, 22.67, 14.17. MS (ESI-TOF) for  $\text{C}_{14}\text{H}_{17}\text{BrN}_2$  [ $\text{M} + \text{H}$ ] $^+$  calculated 293.0648, found 293.0669.

**8-Bromo-3-pentylquinolin-2-amine (29).** Compound **26** was used as reagent. Pale yellow solid (250 mg, 85%).  $^1\text{H}$  NMR (500 MHz,  $\text{CDCl}_3$ )  $\delta$  7.82 (dd,  $J = 1.4, 7.5$  Hz, 1H), 7.65 (s, 1H), 7.55 (dd,  $J = 1.4, 7.9$  Hz, 1H), 7.08 (t,  $J = 7.7$  Hz, 1H), 5.04 (s, 2H), 2.58 (t,  $J = 7.5$  Hz, 2H), 1.78–1.65 (m, 2H), 1.48–1.30 (m, 4H), 0.92 (t,  $J = 7.0$  Hz, 3H).  $^{13}\text{C}$  NMR (126 MHz,  $\text{CDCl}_3$ )  $\delta$  157.09, 143.79, 135.84, 132.41, 126.93, 125.67, 124.65, 122.94, 120.61, 31.76, 31.08, 27.58, 22.67, 14.16. MS (ESI-TOF) for  $\text{C}_{14}\text{H}_{17}\text{BrN}_2$  [ $\text{M} + \text{H}$ ] $^+$  calculated 293.0648, found 293.0675.

**Compounds 30a–c, 31a–c, 32a–c, and 33.** They were synthesized similarly as compound **17a**.

**4-(2-Amino-3-pentylquinolin-5-yl)butanenitrile (30a).** Compound **16** and 3-cyanopropylzinc bromide were used as reagents. White solid (44 mg, 78%).  $^1\text{H}$  NMR (500 MHz,  $\text{CDCl}_3$ )  $\delta$  7.86 (s, 1H), 7.56 (d,  $J = 8.4$  Hz, 1H), 7.44 (dd,  $J = 7.1, 8.4$  Hz, 1H), 7.10 (dd,  $J = 1.1, 7.1$  Hz, 1H), 4.83 (s, 2H), 3.15 (t,  $J = 7.4$  Hz, 2H), 2.62 (t,  $J = 7.7$  Hz, 2H), 2.36 (t,  $J = 7.0$  Hz, 2H), 2.12–2.01 (m, 2H), 1.79–1.68 (m, 2H), 1.45–1.37 (m, 4H), 0.93 (t,  $J = 7.0$  Hz, 3H).  $^{13}\text{C}$  NMR (126 MHz,  $\text{CDCl}_3$ )  $\delta$  155.95, 147.16, 135.47, 131.33, 128.61, 125.08, 123.79, 123.28, 122.75, 119.71, 31.84, 31.77, 31.02, 27.95, 26.64, 22.66, 16.84, 14.21. MS (ESI-TOF) for  $\text{C}_{18}\text{H}_{23}\text{N}_3$  [ $\text{M} + \text{H}$ ] $^+$  calculated 282.1965, found 282.1904.

**5-(2-Amino-3-pentylquinolin-5-yl)pentanenitrile (30b).** Compound **16** and 4-cyanobutylzinc bromide were used as reagents. Off-white solid (45 mg, 76%).  $^1\text{H}$  NMR (500 MHz,  $\text{CDCl}_3$ )  $\delta$  7.84 (s, 1H), 7.54 (d,  $J = 8.4$  Hz, 1H), 7.43 (dd,  $J = 7.1, 8.4$  Hz, 1H), 7.07 (dd,  $J = 1.1, 7.1$  Hz, 1H), 4.80 (s, 2H), 3.02 (t,  $J = 7.5$  Hz, 2H), 2.62 (t,  $J = 7.6$  Hz, 2H), 2.37 (t,  $J = 7.1$  Hz, 2H), 1.93–1.83 (m, 2H), 1.80–1.69 (m, 4H), 1.47–1.36 (m, 4H), 0.93 (t,  $J = 7.1$  Hz, 3H).  $^{13}\text{C}$  NMR (126 MHz,  $\text{CDCl}_3$ )  $\delta$  155.86, 147.12, 136.99, 131.59, 128.56, 124.66, 123.49, 123.01, 122.83, 119.68, 31.82, 31.77, 31.69, 29.93, 27.97, 25.25, 22.67, 17.27, 14.22. MS (ESI-TOF) for  $\text{C}_{19}\text{H}_{25}\text{N}_3$  [ $\text{M} + \text{H}$ ] $^+$  calculated 296.2121, found 296.2068.

**6-(2-Amino-3-pentylquinolin-5-yl)hexanenitrile (30c).** Compound **16** and 5-cyanopentylzinc bromide were used as reagents. White solid (38 mg, 61%).  $^1\text{H}$  NMR (500 MHz,  $\text{CDCl}_3$ )  $\delta$  7.84 (s, 1H), 7.53 (d,  $J = 8.4$  Hz, 1H), 7.42 (dd,  $J = 7.1, 8.4$  Hz, 1H), 7.07 (dd,  $J = 1.2, 7.0$  Hz, 1H), 4.80 (s, 2H), 2.99 (t,  $J = 7.6$  Hz, 2H), 2.62 (t,  $J = 7.7$  Hz, 2H), 2.34 (t,  $J = 7.1$  Hz, 2H), 1.80–1.64 (m, 6H), 1.62–1.53 (m, 2H), 1.45–1.36 (m, 4H), 0.93 (t,  $J = 7.0$  Hz, 3H).  $^{13}\text{C}$  NMR (126 MHz,  $\text{CDCl}_3$ )  $\delta$  155.81, 147.02, 137.81, 131.78, 128.58, 124.38, 123.33, 122.91, 122.86, 119.84, 32.30, 31.79, 31.75, 30.36, 28.78, 27.98, 25.48, 22.68, 17.29, 14.22. MS (ESI-TOF) for  $\text{C}_{20}\text{H}_{27}\text{N}_3$  [ $\text{M} + \text{H}$ ] $^+$  calculated 310.2278, found 310.2323.

**4-(2-Amino-3-pentylquinolin-6-yl)butanenitrile (31a).** Compound **27** and 3-cyanopropylzinc bromide were used as reagents. White solid (35 mg, 62%).  $^1\text{H}$  NMR (500 MHz,  $\text{CDCl}_3$ )  $\delta$  7.64 (s, 1H), 7.60 (d,  $J = 8.5$  Hz, 1H), 7.41 (d,  $J = 2.0$  Hz, 1H), 7.34 (dd,  $J = 2.1, 8.5$  Hz, 1H), 4.80 (s, 2H), 2.89 (t,  $J = 7.3$  Hz, 2H), 2.58 (t,  $J = 7.7$  Hz, 2H), 2.33 (t,  $J = 7.1$  Hz, 2H), 2.13–1.95 (m, 2H), 1.79–1.65 (m, 2H), 1.45–1.36 (m, 4H), 0.93 (t,  $J = 7.1$  Hz, 3H).  $^{13}\text{C}$  NMR (126 MHz,  $\text{CDCl}_3$ )  $\delta$  156.14, 145.35, 135.19, 133.81, 129.65, 126.26, 126.06, 124.58, 124.15, 119.73, 34.18, 31.80, 31.31, 27.71, 27.02, 22.69, 16.47, 14.19. MS (ESI-TOF) for  $\text{C}_{18}\text{H}_{23}\text{N}_3$  [ $\text{M} + \text{H}$ ] $^+$  calculated 282.1965, found 282.1832.

**5-(2-Amino-3-pentylquinolin-6-yl)pentanenitrile (31b).** Compound **27** and 4-cyanobutylzinc bromide were used as reagents. Pale yellow solid (39 mg, 66%).  $^1\text{H}$  NMR (500 MHz,  $\text{CDCl}_3$ )  $\delta$  7.63 (s, 1H), 7.59 (d,  $J = 8.5$  Hz, 1H), 7.37 (d,  $J = 1.9$  Hz, 1H), 7.34 (dd,  $J = 2.1, 8.5$  Hz, 1H), 4.78 (s, 2H), 2.76 (t,  $J = 7.4$  Hz, 2H), 2.57 (t,  $J = 7.8$  Hz, 2H), 2.36 (t,  $J = 7.1$  Hz, 2H), 1.89–1.80 (m, 2H), 1.76–1.69

(m, 4H), 1.48–1.30 (m, 4H), 0.93 (t,  $J = 7.0$  Hz, 3H).  $^{13}\text{C}$  NMR (126 MHz,  $\text{CDCl}_3$ )  $\delta$  155.97, 145.13, 135.46, 135.22, 129.91, 125.82, 125.76, 124.56, 123.98, 119.80, 34.84, 31.80, 31.32, 30.41, 27.74, 24.96, 22.70, 17.26, 14.19. MS (ESI-TOF) for  $\text{C}_{19}\text{H}_{25}\text{N}_3$  [ $\text{M} + \text{H}$ ] $^+$  calculated 296.2121, found 296.2146.

**6-(2-Amino-3-pentylquinolin-6-yl)hexanenitrile (31c).** Compound **27** and 5-cyanopentylzinc bromide were used as reagents. Pale yellow solid (40 mg, 65%).  $^1\text{H}$  NMR (500 MHz,  $\text{CDCl}_3$ )  $\delta$  7.63 (s, 1H), 7.58 (d,  $J = 8.5$  Hz, 1H), 7.37 (d,  $J = 1.9$  Hz, 1H), 7.34 (dd,  $J = 2.1, 8.5$  Hz, 1H), 4.77 (s, 2H), 2.73 (t,  $J = 7.6$  Hz, 2H), 2.57 (t,  $J = 7.7$  Hz, 2H), 2.33 (t,  $J = 7.1$  Hz, 2H), 1.78–1.61 (m, 6H), 1.56–1.46 (m, 2H), 1.44–1.36 (m, 4H), 0.93 (t,  $J = 7.0$  Hz, 3H).  $^{13}\text{C}$  NMR (126 MHz,  $\text{CDCl}_3$ )  $\delta$  155.89, 145.03, 136.28, 135.24, 130.01, 125.75, 125.63, 124.55, 123.88, 119.93, 35.44, 31.81, 31.33, 30.77, 28.42, 27.76, 25.47, 22.70, 17.27, 14.19. MS (ESI-TOF) for  $\text{C}_{20}\text{H}_{27}\text{N}_3$  [ $\text{M} + \text{H}$ ] $^+$  calculated 310.2278, found 310.2309.

**4-(2-Amino-3-pentylquinolin-7-yl)butanenitrile (32a).** Compound **28** and 3-cyanopropylzinc bromide were used as reagents. Pale yellow solid (33 mg, 59%).  $^1\text{H}$  NMR (500 MHz,  $\text{CDCl}_3$ )  $\delta$  7.66 (s, 1H), 7.55 (d,  $J = 8.1$  Hz, 1H), 7.45 (s, 1H), 7.09 (dd,  $J = 1.7, 8.1$  Hz, 1H), 4.83 (s, 2H), 2.91 (t,  $J = 7.3$  Hz, 2H), 2.57 (t,  $J = 7.6$  Hz, 2H), 2.34 (t,  $J = 7.1$  Hz, 2H), 2.12–2.02 (m, 2H), 1.78–1.68 (m, 2H), 1.51–1.31 (m, 4H), 0.93 (t,  $J = 7.0$  Hz, 3H).  $^{13}\text{C}$  NMR (126 MHz,  $\text{CDCl}_3$ )  $\delta$  156.54, 146.63, 140.61, 135.31, 127.40, 124.69, 123.73, 123.46, 123.24, 119.70, 34.72, 31.80, 31.27, 27.73, 26.85, 22.69, 16.52, 14.19. MS (ESI-TOF) for  $\text{C}_{18}\text{H}_{23}\text{N}_3$  [ $\text{M} + \text{H}$ ] $^+$  calculated 282.1965, found 282.1978.

**5-(2-Amino-3-pentylquinolin-7-yl)pentanenitrile (32b).** Compound **28** and 4-cyanobutylzinc bromide were used as reagents. Off-white solid (36 mg, 61%).  $^1\text{H}$  NMR (500 MHz,  $\text{CDCl}_3$ )  $\delta$  7.66 (s, 1H), 7.54 (d,  $J = 8.1$  Hz, 1H), 7.43 (s, 1H), 7.09 (dd,  $J = 1.7, 8.2$  Hz, 1H), 4.81 (s, 2H), 2.79 (t,  $J = 7.4$  Hz, 2H), 2.57 (t,  $J = 7.6$  Hz, 2H), 2.34 (t,  $J = 7.1$  Hz, 2H), 1.94–1.81 (m, 2H), 1.77–1.63 (m, 4H), 1.45–1.36 (m, 4H), 0.93 (t, 3H).  $^{13}\text{C}$  NMR (126 MHz,  $\text{CDCl}_3$ )  $\delta$  156.44, 146.56, 142.18, 135.36, 127.15, 124.52, 123.82, 123.20, 123.00, 119.77, 35.26, 31.80, 31.26, 30.06, 27.75, 24.87, 22.69, 17.22, 14.19. MS (ESI-TOF) for  $\text{C}_{19}\text{H}_{25}\text{N}_3$  [ $\text{M} + \text{H}$ ] $^+$  calculated 296.2121, found 296.2168.

**6-(2-Amino-3-pentylquinolin-7-yl)hexanenitrile (32c).** Compound **28** and 5-cyanopentylzinc bromide were used as reagents. Pale yellow solid (39 mg, 63%). MS (ESI-TOF) for  $\text{C}_{20}\text{H}_{27}\text{N}_3$  [ $\text{M} + \text{H}$ ] $^+$  calculated 310.2278, found 310.2309.

**4-(2-Amino-3-pentylquinolin-8-yl)butanenitrile (33).** Compound **29** and 3-cyanopropylzinc bromide were used as reagents. Pale yellow solid (30 mg, 53%).  $^1\text{H}$  NMR (500 MHz,  $\text{CDCl}_3$ )  $\delta$  7.66 (s, 1H), 7.49 (dd,  $J = 1.5, 8.0$  Hz, 1H), 7.35 (dd,  $J = 1.4, 7.1$  Hz, 1H), 7.16 (dd,  $J = 7.1, 8.0$  Hz, 1H), 4.79 (s, 2H), 3.23 (t,  $J = 7.0$  Hz, 2H), 2.58 (t,  $J = 7.6$  Hz, 2H), 2.32 (t,  $J = 7.1$  Hz, 2H), 2.19–2.09 (m, 2H), 1.79–1.66 (m, 2H), 1.45–1.33 (m, 4H), 0.93 (t,  $J = 7.1$  Hz, 3H).  $^{13}\text{C}$  NMR (126 MHz,  $\text{CDCl}_3$ )  $\delta$  155.58, 145.03, 135.76, 135.33, 128.76, 125.91, 124.72, 123.64, 122.30, 120.54, 31.83, 31.28, 30.49, 27.78, 26.53, 22.70, 16.95, 14.19. MS (ESI-TOF) for  $\text{C}_{18}\text{H}_{23}\text{N}_3$  [ $\text{M} + \text{H}$ ] $^+$  calculated 282.1965, found 282.2008.

**Compounds 34a–c.** They were synthesized similarly as compound **18a**.

**5-(4-Aminobutyl)-3-pentylquinolin-2-amine (34a).** Compound **30a** was used as reagent. White solid (20 mg, 70%).  $^1\text{H}$  NMR (500 MHz, MeOD)  $\delta$  7.95 (s, 1H), 7.42–7.35 (m, 2H), 7.08 (dd,  $J = 3.1, 5.1$  Hz, 1H), 3.00 (t,  $J = 7.6$  Hz, 2H), 2.69–2.63 (m, 4H), 1.78–1.64 (m, 4H), 1.61–1.50 (m, 2H), 1.46–1.40 (m, 4H), 0.95 (t,  $J = 7.0$  Hz, 3H).  $^{13}\text{C}$  NMR (126 MHz, MeOD)  $\delta$  157.97, 147.47, 139.74, 133.37, 129.56, 125.18, 123.77, 123.64, 123.41, 42.51, 33.75, 33.21, 32.72, 32.07, 29.82, 29.05, 23.68, 14.47. MS (ESI-TOF) for  $\text{C}_{18}\text{H}_{27}\text{N}_3$  [ $\text{M} + \text{H}$ ] $^+$  calculated 286.2278, found 286.2218.

**5-(5-Aminopentyl)-3-pentylquinolin-2-amine (34b).** Compound **30b** was used as reagent. White solid (21 mg, 70%).  $^1\text{H}$  NMR (500 MHz, MeOD)  $\delta$  7.94 (s, 1H), 7.42–7.32 (m, 2H), 7.06 (dd,  $J = 2.9, 5.4$  Hz, 1H), 2.98 (t,  $J = 7.6$  Hz, 2H), 2.67 (t,  $J = 7.6$  Hz, 2H), 2.62 (t,  $J = 7.0$  Hz, 2H), 1.78–1.65 (m, 4H), 1.57–1.47 (m, 2H), 1.49–1.39 (m, 6H), 0.95 (t,  $J = 7.0$  Hz, 3H).  $^{13}\text{C}$  NMR (126 MHz,

MeOD)  $\delta$  157.96, 147.46, 139.91, 133.37, 129.57, 125.12, 123.73, 123.58, 123.39, 42.53, 33.77, 33.35, 32.69, 32.39, 32.04, 29.03, 27.94, 23.68, 14.47. MS (ESI-TOF) for  $C_{19}H_{29}N_3$  [M + H]<sup>+</sup> calculated 300.2434, found 300.2374.

**5-(6-Aminoheptyl)-3-pentylquinolin-2-amine (34c).** Compound **30c** was used as reagent. White solid (18 mg, 57%). <sup>1</sup>H NMR (500 MHz, MeOD)  $\delta$  7.95 (s, 1H), 7.41–7.32 (m, 2H), 7.06 (dd, *J* = 3.0, 5.3 Hz, 1H), 2.98 (t, *J* = 7.6 Hz, 2H), 2.67 (t, *J* = 7.4 Hz, 2H), 2.63 (t, *J* = 7.0 Hz, 2H), 1.71 (dq, *J* = 7.8, 15.5 Hz, 4H), 1.50–1.37 (m, 10H), 0.95 (t, *J* = 7.0 Hz, 3H). <sup>13</sup>C NMR (126 MHz, MeOD)  $\delta$  157.96, 147.45, 140.00, 133.37, 129.56, 125.08, 123.72, 123.55, 123.39, 42.40, 33.46, 33.34, 32.68, 32.51, 32.00, 30.48, 28.99, 27.93, 23.68, 14.47. MS (ESI-TOF) for  $C_{20}H_{31}N_3$  [M + H]<sup>+</sup> calculated 314.2591, found 314.2537.

**4-(2-Amino-3-pentylquinolin-5-yl)butanamide (34d).** Compound **34d** was synthesized similarly as compound **18d**. Compound **30a** was used as reagent. White solid (15 mg, 50%). <sup>1</sup>H NMR (500 MHz, MeOD)  $\delta$  8.02 (s, 1H), 7.45–7.31 (m, 2H), 7.08 (dd, *J* = 2.9, 5.4 Hz, 1H), 3.01 (t, *J* = 7.7 Hz, 2H), 2.68 (t, *J* = 7.7 Hz, 2H), 2.30 (t, *J* = 7.3 Hz, 2H), 2.03–1.91 (m, 2H), 1.80–1.66 (m, 2H), 1.48–1.38 (m, 4H), 0.94 (t, *J* = 7.0 Hz, 3H). <sup>13</sup>C NMR (126 MHz, MeOD)  $\delta$  178.76, 157.96, 147.27, 139.18, 133.57, 129.64, 125.45, 123.92, 123.69, 123.43, 35.95, 32.85, 32.76, 32.13, 29.12, 28.38, 23.68, 14.47. MS (ESI-TOF) for  $C_{18}H_{25}N_3O$  [M + H]<sup>+</sup> calculated 300.2070, found 300.2025.

**1-(4-(2-Amino-3-pentylquinolin-5-yl)butyl)guanidine (34e).** 1H-Pyrazole-1-carboxamide hydrochloride (16 mg, 0.11 mmol) and Et<sub>3</sub>N (15.3  $\mu$ L, 0.11 mmol) were added to a solution of compound **34a** (28.5 mg, 0.1 mmol) in MeOH (2 mL), and the reaction mixture was stirred for 3 h at room temperature. The solvent was removed under reduced pressure and the crude material was purified by basic-alumina column chromatography (30% MeOH/CH<sub>2</sub>Cl<sub>2</sub>) to obtain **34e** as a white solid (16 mg, 49%). <sup>1</sup>H NMR (500 MHz, DMSO-*d*<sub>6</sub>)  $\delta$  7.82 (s, 1H), 7.60 (t, *J* = 5.7 Hz, 1H), 7.36–7.24 (m, 3H), 6.98 (dd, *J* = 3.1, 5.3 Hz, 1H), 6.84 (s, 2H), 6.22 (s, 2H), 3.13 (q, *J* = 6.9 Hz, 2H), 2.92 (t, *J* = 7.5 Hz, 2H), 2.60 (t, *J* = 7.6 Hz, 2H), 1.68–1.56 (m, 4H), 1.58–1.46 (m, 2H), 1.39–1.29 (m, 4H), 0.88 (t, *J* = 7.0 Hz, 3H). <sup>13</sup>C NMR (126 MHz, DMSO-*d*<sub>6</sub>)  $\delta$  156.72, 156.66, 146.95, 137.62, 130.71, 127.62, 123.66, 123.27, 121.56, 121.26, 40.52, 31.08, 30.96, 30.56, 28.36, 27.64, 27.62, 22.03, 14.00. MS (ESI-TOF) for  $C_{19}H_{29}N_5$  [M + H]<sup>+</sup> calculated 328.2496, found 328.2444.

**Compounds 35a–c, 36a–c, and 37.** They were synthesized similarly as compound **18a**.

**6-(4-Aminobutyl)-3-pentylquinolin-2-amine (35a).** Compound **31a** was used as reagent. White solid (16 mg, 56%). <sup>1</sup>H NMR (500 MHz, MeOD)  $\delta$  7.70 (s, 1H), 7.48–7.40 (m, 2H), 7.36 (dd, *J* = 2.0, 8.5 Hz, 1H), 2.73 (t, *J* = 7.5 Hz, 2H), 2.66 (t, *J* = 7.3 Hz, 2H), 2.62 (t, *J* = 7.5 Hz, 2H), 1.76–1.66 (m, 4H), 1.57–1.47 (m, 2H), 1.46–1.39 (m, 4H), 0.94 (t, *J* = 7.1 Hz, 3H). <sup>13</sup>C NMR (126 MHz, MeOD)  $\delta$  158.06, 145.47, 137.66, 136.72, 131.08, 126.94, 125.75, 125.30, 124.97, 42.38, 36.34, 33.20, 32.78, 31.81, 29.96, 28.96, 23.68, 14.43. MS (ESI-TOF) for  $C_{18}H_{27}N_3$  [M + H]<sup>+</sup> calculated 286.2278, found 286.2283.

**6-(5-Aminopentyl)-3-pentylquinolin-2-amine (35b).** Compound **31b** was used as reagent. Off-white solid (19 mg, 63%). <sup>1</sup>H NMR (500 MHz, MeOD)  $\delta$  7.70 (s, 1H), 7.45 (d, *J* = 8.5 Hz, 1H), 7.41 (s, 1H), 7.35 (dd, *J* = 2.0, 8.5 Hz, 1H), 2.72 (t, *J* = 7.6 Hz, 2H), 2.66–2.58 (m, 4H), 1.76–1.65 (m, 4H), 1.55–1.48 (m, 2H), 1.47–1.35 (m, 6H), 0.95 (t, *J* = 6.9 Hz, 3H). <sup>13</sup>C NMR (126 MHz, MeOD)  $\delta$  158.03, 145.42, 137.86, 136.72, 131.09, 126.88, 125.73, 125.30, 124.92, 42.50, 36.48, 33.66, 32.80, 32.61, 31.82, 28.97, 27.61, 23.68, 14.43. MS (ESI-TOF) for  $C_{19}H_{29}N_3$  [M + H]<sup>+</sup> calculated 300.2434, found 300.2487.

**6-(6-Aminoheptyl)-3-pentylquinolin-2-amine (35c).** Compound **31c** was used as reagent. Off-white solid (20 mg, 64%). <sup>1</sup>H NMR (500 MHz, MeOD)  $\delta$  7.70 (s, 1H), 7.44 (d, *J* = 8.5 Hz, 1H), 7.40 (s, 1H), 7.34 (dd, *J* = 2.0, 8.5 Hz, 1H), 2.70 (t, *J* = 7.6 Hz, 2H), 2.65–2.57 (m, 4H), 1.76–1.62 (m, 4H), 1.49–1.33 (m, 10H), 0.94 (t, *J* = 7.0 Hz, 3H). <sup>13</sup>C NMR (126 MHz, MeOD)  $\delta$  158.02, 145.41, 137.96, 136.71, 131.10, 126.86, 125.72, 125.30, 124.90, 42.52, 36.50,

33.73, 32.80, 32.70, 31.83, 30.18, 28.97, 27.89, 23.68, 14.44. MS (ESI-TOF) for  $C_{20}H_{31}N_3$  [M + H]<sup>+</sup> calculated 314.2591, found 314.2649.

**7-(4-Aminobutyl)-3-pentylquinolin-2-amine (36a).** Compound **32a** was used as reagent. Off-white solid (19 mg, 67%). <sup>1</sup>H NMR (500 MHz, MeOD)  $\delta$  7.71 (s, 1H), 7.53 (d, *J* = 8.1 Hz, 1H), 7.33 (s, 1H), 7.10 (dd, *J* = 1.7, 8.2 Hz, 1H), 2.75 (t, *J* = 7.6 Hz, 2H), 2.65 (t, *J* = 7.2 Hz, 2H), 2.61 (t, *J* = 7.6 Hz, 2H), 1.78–1.65 (m, 4H), 1.58–1.48 (m, 2H), 1.46–1.39 (m, 4H), 0.94 (t, *J* = 7.0 Hz, 3H). <sup>13</sup>C NMR (126 MHz, MeOD)  $\delta$  158.52, 147.11, 144.79, 136.77, 128.05, 124.90, 124.62, 123.96, 123.62, 42.44, 36.97, 33.45, 32.77, 31.75, 29.78, 28.97, 23.68, 14.42. MS (ESI-TOF) for  $C_{18}H_{27}N_3$  [M + H]<sup>+</sup> calculated 286.2278, found 286.2287.

**7-(5-Aminopentyl)-3-pentylquinolin-2-amine (36b).** Compound **32b** was used as reagent. White solid (18 mg, 60%). <sup>1</sup>H NMR (500 MHz, MeOD)  $\delta$  7.71 (s, 1H), 7.53 (d, *J* = 8.1 Hz, 1H), 7.32 (s, 1H), 7.08 (dd, *J* = 1.7, 8.1 Hz, 1H), 2.74 (t, *J* = 7.6 Hz, 2H), 2.65–2.58 (m, 4H), 1.76–1.66 (m, 4H), 1.56–1.47 (m, 2H), 1.46–1.36 (m, 6H), 0.94 (t, *J* = 7.0 Hz, 3H). <sup>13</sup>C NMR (126 MHz, MeOD)  $\delta$  158.52, 147.10, 144.96, 136.78, 128.02, 124.88, 124.64, 123.90, 123.58, 42.47, 37.08, 33.62, 32.78, 32.38, 31.75, 28.97, 27.62, 23.68, 14.43. MS (ESI-TOF) for  $C_{19}H_{29}N_3$  [M + H]<sup>+</sup> calculated 300.2434, found 300.2486.

**7-(6-Aminoheptyl)-3-pentylquinolin-2-amine (36c).** Compound **32c** was used as reagent. White solid (20 mg, 64%). <sup>1</sup>H NMR (500 MHz, MeOD)  $\delta$  7.71 (d, *J* = 0.9 Hz, 1H), 7.53 (d, *J* = 8.2 Hz, 1H), 7.32 (s, 1H), 7.08 (dd, *J* = 1.7, 8.1 Hz, 1H), 2.73 (t, *J* = 7.6 Hz, 2H), 2.66–2.56 (m, 4H), 1.78–1.65 (m, 4H), 1.55–1.35 (m, 10H), 0.94 (t, *J* = 7.1 Hz, 3H). <sup>13</sup>C NMR (126 MHz, MeOD)  $\delta$  158.50, 147.09, 145.03, 136.78, 128.00, 124.86, 124.65, 123.89, 123.56, 42.40, 37.07, 33.42, 32.79, 32.43, 31.75, 30.14, 28.98, 27.85, 23.69, 14.43. MS (ESI-TOF) for  $C_{20}H_{31}N_3$  [M + H]<sup>+</sup> calculated 314.2591, found 314.2646.

**8-(4-Aminobutyl)-3-pentylquinolin-2-amine (37).** Compound **33** was used as reagent. White solid (17 mg, 60%). <sup>1</sup>H NMR (500 MHz, MeOD)  $\delta$  7.68 (s, 1H), 7.44 (dd, *J* = 1.5, 8.0 Hz, 1H), 7.32 (dd, *J* = 1.4, 7.1 Hz, 1H), 7.10 (dd, *J* = 7.1, 8.0 Hz, 1H), 3.06 (t, *J* = 7.7 Hz, 2H), 2.69 (t, *J* = 7.1 Hz, 2H), 2.62 (t, *J* = 7.7 Hz, 2H), 1.81–1.68 (m, 4H), 1.61–1.51 (m, 2H), 1.46–1.39 (m, 4H), 0.94 (t, *J* = 6.9 Hz, 3H). <sup>13</sup>C NMR (126 MHz, MeOD)  $\delta$  157.96, 145.92, 137.83, 137.02, 129.40, 126.33, 125.61, 125.14, 122.79, 42.40, 33.63, 32.83, 32.10, 31.86, 28.96, 28.93, 23.69, 14.43. MS (ESI-TOF) for  $C_{18}H_{27}N_3$  [M + H]<sup>+</sup> calculated 286.2278, found 286.2283.

**2-Amino-4,6-dibromobenzaldehyde (40).** A solution of compound **38** (737 mg, 2.5 mmol) in THF (20 mL) was added slowly to a solution of LiAlH<sub>4</sub> (10 mL, 10 mmol, 1.0 M in THF) in THF (10 mL) at 0 °C under nitrogen atmosphere. The reaction mixture was stirred for 4 h at 25 °C. The reaction mixture was carefully quenched with ice-cold water (1 mL) at 0 °C, and 10% NaOH (1 mL) was added. The resulting mixture was stirred for 10 min at room temperature, filtered through Celite and washed with CH<sub>2</sub>Cl<sub>2</sub> (50 mL). The resulting filtrate was dried over Na<sub>2</sub>SO<sub>4</sub> and concentrated under reduced pressure and the crude material was purified by flash column chromatography (30% EtOAc/hexanes) to obtain the compound **39** as a off-white solid (386 mg, 55%). MS (ESI-TOF) for  $C_7H_7Br_2NO$  [M + H]<sup>+</sup> calculated 279.8967, found 279.8975. To a solution of compound **39** (351 mg, 1.25 mmol) in CH<sub>2</sub>Cl<sub>2</sub> (10 mL) was added MnO<sub>2</sub> (326 mg, 3.75 mmol, activated). The mixture was stirred for 6 h and then filtered over Celite. The mixture was concentrated and purified by flash chromatography (20% EtOAc/hexanes) to give compound **40** as a yellow solid (286 mg, 82%). <sup>1</sup>H NMR (400 MHz, CDCl<sub>3</sub>)  $\delta$  10.33 (s, 1H), 7.07 (d, *J* = 1.8 Hz, 1H), 6.81 (d, *J* = 1.1 Hz, 1H), 6.56 (s, 2H). <sup>13</sup>C NMR (126 MHz, CDCl<sub>3</sub>)  $\delta$  194.69, 152.20, 130.08, 129.98, 124.03, 118.97, 113.96. MS (ESI-TOF) for  $C_7H_5Br_2NO$  [M + H]<sup>+</sup> calculated 277.8811, found 277.8811.

**5,7-Dibromo-3-pentylquinolin-2-amine (41).** Compound **41** was synthesized similarly as compound **16**. Compound **40** was used as reagent. Off-white solid (242 mg, 65%). <sup>1</sup>H NMR (400 MHz, CDCl<sub>3</sub>)  $\delta$  7.96 (s, 1H), 7.77 (dd, *J* = 0.8, 1.9 Hz, 1H), 7.61 (d, *J* = 1.9 Hz, 1H), 4.98 (s, 2H), 2.58 (t, *J* = 7.6 Hz, 2H), 1.81–1.68 (m, 2H), 1.48–1.36 (m, 4H), 0.94 (t, *J* = 7.0 Hz, 3H). <sup>13</sup>C NMR (126 MHz, CDCl<sub>3</sub>)  $\delta$

157.24, 147.77, 134.54, 128.98, 128.00, 125.45, 122.50, 121.99, 121.86, 31.78, 31.35, 27.55, 22.65, 14.18. MS (ESI-TOF) for  $C_{14}H_{16}Br_2N_2$  [ $M + H$ ]<sup>+</sup> calculated 370.9753, found 370.9747.

**5,5'-(2-Amino-3-pentylquinoline-5,7-diyl)bis(pentan-1-amine) (43).** To a solution of compound 41 (74 mg, 0.2 mmol) in THF (2 mL) were added 4-cyanobutylzinc bromide (1.6 mL, 0.8 mmol, 0.5 M in THF) and Pd(PPh<sub>3</sub>)<sub>4</sub> (23 mg, 0.02 mmol). The resulting reaction mixture was stirred at 65 °C under nitrogen atmosphere for 24 h. The reaction mixture was diluted with water and extracted with EtOAc (3 × 10 mL). The combined organic layer was dried over Na<sub>2</sub>SO<sub>4</sub> and concentrated under reduced pressure. The crude material was purified by flash chromatography (20% MeOH/CH<sub>2</sub>Cl<sub>2</sub>) to obtain the compound 42 as a pale yellow solid (19 mg, 25%). MS (ESI-TOF) for  $C_{24}H_{32}N_4$  [ $M + H$ ]<sup>+</sup> calculated 377.2700, found 377.2691. A solution of compound 42 (19 mg, 0.05 mmol) in THF (5 mL) was added slowly to a solution of LiAlH<sub>4</sub> (0.5 mL, 0.5 mmol, 1.0 M in THF) in THF (3 mL) at 0 °C under nitrogen atmosphere. The reaction mixture was stirred for 2 h at 25 °C and 2 h at 60 °C. The reaction mixture was carefully quenched with ice-cold water (1 mL) at 0 °C, and 10% NaOH (1 mL) was added. The resulting mixture was stirred for 10 min at room temperature, filtered through Celite, and washed with CH<sub>2</sub>Cl<sub>2</sub> (25 mL). The resulting filtrate was dried over Na<sub>2</sub>SO<sub>4</sub> and concentrated under reduced pressure and the crude material was purified by semipreparative reverse phase HPLC to obtain the compound 43 as a white solid (5 mg, 26%). <sup>1</sup>H NMR (400 MHz, MeOD) δ 8.33 (s, 1H), 7.39 (s, 1H), 7.28 (s, 1H), 3.07 (t, *J* = 7.7 Hz, 2H), 2.94 (t, *J* = 7.6 Hz, 4H), 2.86–2.73 (m, 4H), 1.82–1.66 (m, 10H), 1.58–1.40 (m, 8H), 0.95 (t, *J* = 6.8 Hz, 3H). <sup>13</sup>C NMR (126 MHz, MeOD) δ 154.80, 148.71, 141.75, 138.97, 136.98, 128.10, 125.79, 119.63, 115.24, 40.68, 40.68, 36.73, 32.74, 32.45, 32.12, 31.61, 30.84, 29.02, 28.52, 28.42, 27.37, 27.14, 23.63, 14.44. MS (ESI-TOF) for  $C_{24}H_{40}N_4$  [ $M + H$ ]<sup>+</sup> calculated 385.3326, found 385.3330.

**Protein Expression, Purification, and Crystallization.** The extracellular domain of human TLR8 (hTLR8, residues 27–827) was prepared as described previously<sup>74</sup> and was concentrated to 16 mg/mL in 10 mM MES (pH 5.5), 50 mM NaCl. The protein solutions for the crystallization of hTLR8/compound complexes contained hTLR8 (8.5 mg/mL) and compound (protein/compound molar ratio of 1:10) in a crystallization buffer containing 7 mM MES (pH 5.5), 35 mM NaCl. Crystallization experiments were performed with sitting-drop vapor-diffusion methods at 293 K. Crystals of hTLR8/compound were obtained with reservoir solutions containing 9–12% (w/v) PEG3350, 0.3 M potassium formate, and 0.1 M sodium citrate (pH 4.8–5.2).

**Data Collection and Structure Determination.** Diffraction data sets were collected on beamlines PF-AR NE3A (Ibaraki, Japan) and SPring-8 BL41XU under cryogenic conditions at 100 K. Crystals of hTLR8/compound were soaked into a cryoprotectant solution containing 15% (w/v) PEG3350, 0.23 M potassium formate, 75 mM sodium citrate, pH 4.8–5.2, 7.5 mM MES pH 5.5, 38 mM NaCl, and 25% glycerol. Data sets were processed using the HKL2000 package<sup>75</sup> or imosflm.<sup>76</sup> hTLR8/compound structures were determined by the molecular replacement method using the Molrep program<sup>77</sup> with the hTLR8/CL097 structure (PDB code 3W3J) as a search model. The model was further refined with stepwise cycles of manual model building using the COOT program<sup>78</sup> and restrained refinement using REFMAC<sup>79</sup> until the *R* factor was converged. Compound molecule, *N*-glycans, and water molecules were modeled into the electron density maps at the latter cycles of the refinement. The quality of the final structure was evaluated with PROCHECK.<sup>80</sup> The statistics of the data collection and refinement are also summarized in Table S1. The figures representing structures were prepared with PyMOL (Schrödinger, New York, NY). Coordinates have been deposited in the Protein Data Bank of the Research Collaboratory for Structural Bioinformatics; PDB codes for compounds 1 and 2 are, respectively, SAWD and SAWB.

**Human TLR8-Specific Reporter Gene Assays (NF-κB Induction) and TLR-2, -3, -4, -5, -7, -9- and NOD-1/NOD-2 Counterscreens.** The induction of NF-κB was quantified using human TLR-2, -3, -4, -5, -7, -8, -9, and NOD-1/NOD-2-specific, rapid-throughput,

liquid handler-assisted reporter gene assays as previously described by us.<sup>31,47,60,61</sup> HEK293 cells stably co-transfected with the appropriate hTLR (or NOD) and secreted alkaline phosphatase (sAP) were maintained in HEK-Blue Selection medium. Stable expression of secreted alkaline phosphatase (sAP) under control of NF-κB/AP-1 promoters is inducible by appropriate TLR/NOD agonists, and extracellular sAP in the supernatant is proportional to NF-κB induction. Reporter cells were incubated at a density of ~10<sup>5</sup> cells/ml in a volume of 80 μL/well, in 384-well, flat-bottomed, cell culture-treated microtiter plates in the presence of graded concentrations of stimuli. sAP was assayed spectrophotometrically using an alkaline phosphatase-specific chromogen (present in HEK-detection medium as supplied by InvivoGen) at 620 nm. None of the compounds were active in the counterscreens (data not shown), confirming specificity for human TLR8.

**Immunoassays for Cytokines.** Fresh human peripheral blood mononuclear cells (hPBMC) were isolated from human blood obtained by venipuncture with informed consent and as per institutional guidelines on Ficoll–Hypaque gradients. Aliquots of PBMCs (10<sup>5</sup> cells in 100 μL/well) were stimulated for 12 h with graded concentrations of test compounds. Supernatants were isolated by centrifugation and were assayed in duplicates using analyte-specific multiplexed cytokine/chemokine bead array assays as reported by us previously.<sup>59</sup>

**Rabbit Immunization and CRM197<sup>72</sup>-Specific Immunoassays.** All experiments were performed at Harlan Laboratories (Indianapolis, IN) in accordance with institutional guidelines. All antigen/adjuvant preparations were entirely aqueous; no liposomal or emulsifying agents were used. Cohorts of adult female New Zealand White rabbits (*n* = 4) were immunized intramuscularly in the flank region with (a) 10 μg of CRM197<sup>72</sup> in 0.2 mL of saline (unadjuvanted control) or (b) 10 μg of CRM197 in 0.2 mL of saline plus 100 μg of lead TLR8 agonists. Preimmune test-bleeds were first obtained via venipuncture of the marginal vein of the ear. Animals were immunized on days 1, 15, and 28. A final test-bleed was performed via the marginal vein of the ear on day 38. Sera were stored at –80 °C until used. CRM197-specific ELISAs were performed in 384-well format using automated liquid handling methods as described by us elsewhere.<sup>32</sup> A precision 2000 liquid handler (Bio-Tek, Winooski, VT) was used for all serial dilution and reagent addition steps, and a Bio-Tek ELx405 384-well plate washer was employed for plate washes; 100 mM phosphate-buffered saline (PBS), pH 7.4, containing 0.1% Tween-20 was used as wash buffer. Nunc-Immuno MaxiSorp (384-well) plates were coated with 30 mL of CRM197 (10 μg/mL) in 100 mM carbonate buffer, pH 9.0, overnight at 4 °C. After 3 washes, the plates were blocked with 3% bovine serum albumin (in PBS, pH 7.4) for 1 h at rt. Serum samples (in quadruplicate) were serially diluted in a separate 384-well plate using the liquid handler, and an amount of 30 μL of the serum dilutions was transferred using the liquid handler, and the plate was incubated at 37 °C for 2 h. The assay plate was washed three times, and 30 μL of 1:10 000 diluted appropriate anti-rabbit immunoglobulin (IgG, γ chain) conjugated with horseradish peroxidase was added to all wells. Following an incubation step at 37 °C for 1 h and three washes, tetramethylbenzidine substrate was added at concentrations recommended by vendor (Sigma). The chromogenic reaction was terminated at 30 min by the addition of 2 M H<sub>2</sub>SO<sub>4</sub>. Plates were then read at 450 nm using a SpectraMax M4 device (Molecular Devices, Sunnyvale, CA).

**Eight-Color Flow-Cytometric Immunostimulation Experiments.** Cell surface marker upregulation was determined by flow cytometry using protocols published by us previously<sup>73</sup> and modified for rapid throughput. Briefly, heparin-anticoagulated whole blood samples were obtained by venipuncture from healthy human volunteers with informed consent and as per guidelines approved by the University of Kansas Human Subjects Experimentation Committee. Serial dilutions of selected compounds were performed using a Bio-Tek Precision 2000 XS liquid handler in sterile 96-well polypropylene plates, to which were added 100 μL aliquots of anticoagulated whole human blood. The plates were incubated at 37 °C for 16 h. Negative (endotoxin free water) controls were included in each experiment. The following fluorochrome-conjugated antibodies were used: CD3-PE,

CD19-FITC, CD56-APC (eBioscience, San Diego, CA), CD14-V500, CD28 PE-Cy7, CD40 V450, CD80 APC-H7, CD86 PerCP-Cy5.5 (Becton-Dickinson Biosciences, San Jose, CA). Following incubation, 2.5  $\mu\text{g}$  of each antibody was added to wells with a liquid handler and incubated at 4 °C in the dark for 60 min. Following staining, erythrocytes were lysed and leukocytes fixed by mixing 200 mL of the samples in 800 mL prewarmed whole blood lyse/fix buffer (Becton-Dickinson Biosciences, San Jose, CA) in 96 deep-well plates. After washing the cells twice at 300 g for 10 min in RPMI, the cells were transferred to a 96-well plate. Flow cytometry was performed using a BD FACSVerser instrument for acquisition on 100 000 gated events. Compensation for spillover was computed for each experiment on singly stained Comp Beads (Becton-Dickinson Biosciences, San Jose, CA). CD28, CD40, CD80, and CD86 activation in the major leukocyte populations, viz., natural killer lymphocytes (NK cells CD3<sup>-</sup>CD56<sup>+</sup>), cytokine-induced killer phenotype (CIK cells CD3<sup>+</sup>CD56<sup>+</sup>), B lymphocytes (CD19<sup>+</sup>CD3<sup>-</sup>), T lymphocytes (CD3<sup>+</sup>CD56<sup>-</sup>), monocytes (CD14<sup>+</sup>), polymorphonuclear cells (CD14<sup>-</sup>) were quantified using FlowJo, version 7.0, software (Treestar, Ashland, OR).

## ■ ASSOCIATED CONTENT

### ■ Supporting Information

The Supporting Information is available free of charge on the ACS Publications website at DOI: 10.1021/acs.jmedchem.5b01087.

Characterization data (<sup>1</sup>H, <sup>13</sup>C, mass spectra), LC-MS analysis results of key precursors and final compounds (PDF)

Molecular formula strings (CSV)

## ■ AUTHOR INFORMATION

### ■ Corresponding Author

\*Address: Department of Medicinal Chemistry, 2-132, Cancer and Cardiovascular Research Building, 2231 6th Street SE, University of Minnesota, Minneapolis, MN 55455. Phone: 612-625-3317. E-mail: sdavid@umn.edu.

### ■ Notes

The authors declare no competing financial interest.

## ■ ACKNOWLEDGMENTS

This work was supported by NIH/NIAID Contracts HSN272200900033C and HHSN272201400056C. Support for NMR instrumentation was provided by NIH Shared Instrumentation Grant S10RR024664 and NSF Major Research Instrumentation Grant 0320648.

## ■ ABBREVIATIONS USED

APC, antigen-presenting cell; CD, cluster of differentiation; EC<sub>50</sub>, half-maximal effective concentration; ESI-TOF, electrospray ionization-time-of-flight; HEK, human embryonic kidney; IFN, interferon; IL, interleukin; MFI, mean fluorescence intensity; MHC, major histocompatibility complex; MPL, monophosphoryl lipid A; NF- $\kappa$ B, nuclear factor  $\kappa$ B; NK, natural killer; NLR, Nodlike receptor; NOD-1 and -2, nucleotide-binding oligomerization domain-containing proteins 1 and 2; PBMC, peripheral blood mononuclear cell; sAP, secreted alkaline phosphatase; Th1, helper T lymphocyte, type 1; Th2, helper T lymphocyte, type 2; TLR, Toll-like receptor; TNF- $\alpha$ , tumor necrosis factor  $\alpha$

## ■ REFERENCES

(1) CDC. Ten great public health achievements—United States, 1900–1999. *MMWR* **1999**, *48*, 241–243.  
(2) Ramon, G. Adjuvant and inductive agents in immunity; principles, experimental study, applications. *Rev. Pathol. Gen. Physiol. Clin.* **1957**, *57*, 1–62.

(3) Ramon, G. The principle of adjuvant and stimulant substances of immunity; its bases; its applications. *C. R. Hebd. Seances Acad. Sci.* **1955**, *241*, 781–784.

(4) Glenny, A. T.; Pope, C. G.; Waddington, H.; Wallace, V. The antigenic value of toxoid precipitated by potassium-alum. *J. Pathol. Bacteriol.* **1926**, *29*, 38–45.

(5) Gupta, R. K.; Siber, G. R. Adjuvants for human vaccines—current status, problems and future prospects. *Vaccine* **1995**, *13*, 1263–1276.

(6) Gupta, R. K. Aluminum compounds as vaccine adjuvants. *Adv. Drug Delivery Rev.* **1998**, *32*, 155–172.

(7) Klein, N. P. Licensed pertussis vaccines in the United States. History and current state. *Hum. Vaccines Immunother.* **2014**, *10*, 2684–2690.

(8) Sheridan, S. L.; Frith, K.; Snelling, T. L.; Grimwood, K.; McIntyre, P. B.; Lambert, S. B. Waning vaccine immunity in teenagers primed with whole cell and acellular pertussis vaccine: recent epidemiology. *Expert Rev. Vaccines* **2014**, *13*, 1081–1106.

(9) Lavine, J. S.; Bjornstad, O. N.; de Blasio, B. F.; Storsaeter, J. Short-lived immunity against pertussis, age-specific routes of transmission, and the utility of a teenage booster vaccine. *Vaccine* **2012**, *30*, 544–551.

(10) Suryadevara, M.; Domachowske, J. B. Prevention of pertussis through adult vaccination. *Hum. Vaccines Immunother.* **2015**, *11*, 1744–1747.

(11) Clark, T. A. Changing pertussis epidemiology: everything old is new again. *J. Infect. Dis.* **2014**, *209*, 978–981.

(12) Cherry, J. D. Epidemic pertussis in 2012—the resurgence of a vaccine-preventable disease. *N. Engl. J. Med.* **2012**, *367*, 785–787.

(13) Zepp, F.; Heining, U.; Mertsola, J.; Bernatowska, E.; Guiso, N.; Roord, J.; Tozzi, A. E.; Van Damme, P. Rationale for pertussis booster vaccination throughout life in Europe. *Lancet Infect. Dis.* **2011**, *11*, 557–570.

(14) Hara, M.; Fukuoka, M.; Tashiro, K.; Ozaki, I.; Ohfuji, S.; Okada, K.; Nakano, T.; Fukushima, W.; Hirota, Y. Pertussis outbreak in university students and evaluation of acellular pertussis vaccine effectiveness in Japan. *BMC Infect. Dis.* **2015**, *15*, 45.

(15) Warfel, J. M.; Zimmerman, L. I.; Merkel, T. J. Acellular pertussis vaccines protect against disease but fail to prevent infection and transmission in a nonhuman primate model. *Proc. Natl. Acad. Sci. U. S. A.* **2014**, *111*, 787–792.

(16) Hoffmann, J.; Akira, S. Innate immunity. *Curr. Opin. Immunol.* **2013**, *25*, 1–3.

(17) Kumagai, Y.; Akira, S. Identification and functions of pattern-recognition receptors. *J. Allergy Clin. Immunol.* **2010**, *125*, 985–992.

(18) Kawai, T.; Akira, S. The role of pattern-recognition receptors in innate immunity: update on Toll-like receptors. *Nat. Immunol.* **2010**, *11*, 373–384.

(19) Loo, Y. M.; Gale, M., Jr. Immune signaling by RIG-I-like receptors. *Immunity* **2011**, *34*, 680–692.

(20) Kersse, K.; Bertrand, M. J.; Lamkanfi, M.; Vandenabeele, P. NOD-like receptors and the innate immune system: coping with danger, damage and death. *Cytokine Growth Factor Rev.* **2011**, *22*, 257–276.

(21) Clarke, T. B.; Weiser, J. N. Intracellular sensors of extracellular bacteria. *Immunol. Rev.* **2011**, *243*, 9–25.

(22) Cottalorda, A.; Verschele, C.; Marçais, A.; Tomkowiak, M.; Musette, P.; Uematsu, S.; Akira, S.; Marvel, J.; Bonnefoy-Berard, N. TLR2 engagement on CD8 T cells lowers the threshold for optimal antigen-induced T cell activation. *Eur. J. Immunol.* **2006**, *36*, 1684–1693.

(23) Xu, W.; Banchereau, J. The antigen presenting cells instruct plasma cell differentiation. *Front. Immunol.* **2014**, *4*, 504.

(24) Germain, R. N.; Jenkins, M. K. In vivo antigen presentation. *Curr. Opin. Immunol.* **2004**, *16*, 120–125.

(25) Itano, A. A.; Jenkins, M. K. Antigen presentation to naive CD4 T cells in the lymph node. *Nat. Immunol.* **2003**, *4*, 733–739.

(26) Catron, D. M.; Itano, A. A.; Pape, K. A.; Mueller, D. L.; Jenkins, M. K. Visualizing the first 50 h of the primary immune response to a soluble antigen. *Immunity* **2004**, *21*, 341–347.

- (27) Johnson, L. A.; Jackson, D. G. Cell traffic and the lymphatic endothelium. *Ann. N. Y. Acad. Sci.* **2008**, *1131*, 119–133.
- (28) Platt, A. M.; Randolph, G. J. Dendritic cell migration through the lymphatic vasculature to lymph nodes. *Adv. Immunol.* **2013**, *120*, 51–68.
- (29) Teijeira, A.; Rouzaut, A.; Melero, I. Initial afferent lymphatic vessels controlling outbound leukocyte traffic from skin to lymph nodes. *Front. Immunol.* **2013**, *4*, 433.
- (30) Teijeira, A.; Russo, E.; Halin, C. Taking the lymphatic route: dendritic cell migration to draining lymph nodes. *Semin. Immunopathol.* **2014**, *36*, 261–274.
- (31) Jenkins, M. K.; Khoruts, A.; Ingulli, E.; Mueller, D. L.; McSorley, S. J.; Reinhardt, R. L.; Itano, A.; Pape, K. A. In vivo activation of antigen-specific CD4 T cells. *Annu. Rev. Immunol.* **2001**, *19*, 23–45.
- (32) Garside, P.; Ingulli, E.; Merica, R. R.; Johnson, J. G.; Noelle, R. J.; Jenkins, M. K. Visualization of specific B and T lymphocyte interactions in the lymph node. *Science* **1998**, *281*, 96–99.
- (33) Miga, A. J.; Masters, S. R.; Durell, B. G.; Gonzalez, M.; Jenkins, M. K.; Maliszewski, C.; Kikutani, H.; Wade, W. F.; Noelle, R. J. Dendritic cell longevity and T cell persistence is controlled by CD154-CD40 interactions. *Eur. J. Immunol.* **2001**, *31*, 959–965.
- (34) Breitfeld, D.; Ohl, L.; Kremmer, E.; Ellwart, J.; Sallusto, F.; Lipp, M.; Forster, R. Follicular B helper T cells express CXC chemokine receptor 5, localize to B cell follicles, and support immunoglobulin production. *J. Exp. Med.* **2000**, *192*, 1545–1552.
- (35) Hale, J. S.; Ahmed, R. Memory T follicular helper CD4 T cells. *Front. Immunol.* **2015**, *6*, 16.
- (36) Crotty, S. A brief history of T cell help to B cells. *Nat. Rev. Immunol.* **2015**, *15*, 185–189.
- (37) Crotty, S. Follicular helper CD4 T cells (TFH). *Annu. Rev. Immunol.* **2011**, *29*, 621–663.
- (38) McHeyzer-Williams, L. J.; Pelletier, N.; Mark, L.; Fazilleau, N.; McHeyzer-Williams, M. G. Follicular helper T cells as cognate regulators of B cell immunity. *Curr. Opin. Immunol.* **2009**, *21*, 266–273.
- (39) Nurieva, R. I.; Chung, Y. Understanding the development and function of T follicular helper cells. *Cell. Mol. Immunol.* **2010**, *7*, 190–197.
- (40) Hauser, A. E.; Muehlinghaus, G.; Manz, R. A.; Cassese, G.; Arce, S.; Debes, G. F.; Hamann, A.; Berek, C.; Lindenau, S.; Doerner, T.; Hiepe, F.; Odendahl, M.; Riemekasten, G.; Krenn, V.; Radbruch, A. Long-lived plasma cells in immunity and inflammation. *Ann. N. Y. Acad. Sci.* **2003**, *987*, 266–269.
- (41) Borghesi, L.; Milcarek, C. From B cell to plasma cell: regulation of V(D)J recombination and antibody secretion. *Immunol. Res.* **2006**, *36*, 27–32.
- (42) Johnson, K.; Shapiro-Shelef, M.; Tunyaplin, C.; Calame, K. Regulatory events in early and late B-cell differentiation. *Mol. Immunol.* **2005**, *42*, 749–761.
- (43) Salunke, D. B.; Shukla, N. M.; Yoo, E.; Crall, B. M.; Balakrishna, R.; Malladi, S. S.; David, S. A. Structure-activity relationships in human Toll-like receptor 2-specific monoacyl lipopeptides. *J. Med. Chem.* **2012**, *55*, 3353–3363.
- (44) Salunke, D. B.; Connelly, S. W.; Shukla, N. M.; Hermanson, A. R.; Fox, L. M.; David, S. A. Design and development of stable, water-soluble, human Toll-like receptor 2 specific monoacyl lipopeptides as candidate vaccine adjuvants. *J. Med. Chem.* **2013**, *56*, 5885–5900.
- (45) Wu, W.; Li, R.; Malladi, S. S.; Warshakoon, H. J.; Kimbrell, M. R.; Amolins, M. W.; Ukani, R.; Datta, A.; David, S. A. Structure-activity relationships in toll-like receptor-2 agonistic diacylthioglycerol lipopeptides. *J. Med. Chem.* **2010**, *53*, 3198–3213.
- (46) Shukla, N. M.; Kimbrell, M. R.; Malladi, S. S.; David, S. A. Regioisomerism-dependent TLR7 agonism and antagonism in an imidazoquinoline. *Bioorg. Med. Chem. Lett.* **2009**, *19*, 2211–2214.
- (47) Shukla, N. M.; Malladi, S. S.; Mutz, C. A.; Balakrishna, R.; David, S. A. Structure-activity relationships in human toll-like receptor 7-active imidazoquinoline analogues. *J. Med. Chem.* **2010**, *53*, 4450–4465.
- (48) Shukla, N. M.; Mutz, C. A.; Ukani, R.; Warshakoon, H. J.; Moore, D. S.; David, S. A. Syntheses of fluorescent imidazoquinoline conjugates as probes of Toll-like receptor 7. *Bioorg. Med. Chem. Lett.* **2010**, *20*, 6384–6386.
- (49) Shukla, N. M.; Lewis, T. C.; Day, T. P.; Mutz, C. A.; Ukani, R.; Hamilton, C. D.; Balakrishna, R.; David, S. A. Toward self-adjuvanting subunit vaccines: model peptide and protein antigens incorporating covalently bound toll-like receptor-7 agonistic imidazoquinolines. *Bioorg. Med. Chem. Lett.* **2011**, *21*, 3232–3236.
- (50) Shukla, N. M.; Malladi, S. S.; Day, V.; David, S. A. Preliminary evaluation of a 3H imidazoquinoline library as dual TLR7/TLR8 antagonists. *Bioorg. Med. Chem.* **2011**, *19*, 3801–3811.
- (51) Shukla, N. M.; Mutz, C. A.; Malladi, S. S.; Warshakoon, H. J.; Balakrishna, R.; David, S. A. Toll-Like Receptor (TLR)-7 and -8 Modulatory Activities of Dimeric Imidazoquinolines. *J. Med. Chem.* **2012**, *55*, 1106–1116.
- (52) Shukla, N. M.; Salunke, D. B.; Balakrishna, R.; Mutz, C. A.; Malladi, S. S.; David, S. A. Potent adjuvanticity of a pure TLR7-agonistic imidazoquinoline dendrimer. *PLoS One* **2012**, *7*, e43612.
- (53) Yoo, E.; Crall, B. M.; Balakrishna, R.; Malladi, S. S.; Fox, L. M.; Hermanson, A. R.; David, S. A. Structure-activity relationships in Toll-like receptor 7 agonistic 1H-imidazo[4,5-c]pyridines. *Org. Biomol. Chem.* **2013**, *11*, 6526–6545.
- (54) Yoo, E.; Salunke, D. B.; Sil, D.; Guo, X.; Salyer, A. C.; Hermanson, A. R.; Kumar, M.; Malladi, S. S.; Balakrishna, R.; Thompson, W. H.; Tanji, H.; Ohto, U.; Shimizu, T.; David, S. A. Determinants of activity at human Toll-like receptors 7 and 8: quantitative structure-activity relationship (QSAR) of diverse heterocyclic scaffolds. *J. Med. Chem.* **2014**, *57*, 7955–7970.
- (55) Salunke, D. B.; Yoo, E.; Shukla, N. M.; Balakrishna, R.; Malladi, S. S.; Serafin, K. J.; Day, V. W.; Wang, X.; David, S. A. Structure-activity relationships in human Toll-like receptor 8-active 2,3-diaminofuro[2,3-c]pyridines. *J. Med. Chem.* **2012**, *55*, 8137–8151.
- (56) Kokatla, H. P.; Yoo, E.; Salunke, D. B.; Sil, D.; Ng, C. F.; Balakrishna, R.; Malladi, S. S.; Fox, L. M.; David, S. A. Toll-like receptor-8 agonistic activities in C2, C4, and C8 modified thiazolo[4,5-c]quinolines. *Org. Biomol. Chem.* **2013**, *11*, 1179–1198.
- (57) Kokatla, H. P.; Sil, D.; Malladi, S. S.; Balakrishna, R.; Hermanson, A. R.; Fox, L. M.; Wang, X.; Dixit, A.; David, S. A. Exquisite selectivity for human toll-like receptor 8 in substituted furo[2,3-c]quinolines. *J. Med. Chem.* **2013**, *56*, 6871–6885.
- (58) Kokatla, H. P.; Sil, D.; Tanji, H.; Ohto, U.; Malladi, S. S.; Fox, L. M.; Shimizu, T.; David, S. A. Structure-based design of novel human Toll-like receptor 8 agonists. *ChemMedChem* **2014**, *9*, 719–723.
- (59) Bees, M.; Malladi, S. S.; Fox, L. M.; Jones, C. D.; Dixit, A.; David, S. A. Human Toll-like receptor 8-selective agonistic activities in 1-alkyl-1H-benzimidazol-2-amines. *J. Med. Chem.* **2014**, *57*, 7325–7341.
- (60) Agnihotri, G.; Ukani, R.; Malladi, S. S.; Warshakoon, H. J.; Balakrishna, R.; Wang, X.; David, S. A. Structure-activity relationships in nucleotide oligomerization domain 1 (Nod1) agonistic gamma-glutamylidiaminopimelic acid derivatives. *J. Med. Chem.* **2011**, *54*, 1490–1510.
- (61) Ukani, R.; Lewis, T. C.; Day, T. P.; Wu, W.; Malladi, S. S.; Warshakoon, H. J.; David, S. A. Potent adjuvantic activity of a CCR1-agonistic bis-quinoline. *Bioorg. Med. Chem. Lett.* **2012**, *22*, 293–295.
- (62) Bekereldjian-Ding, I.; Roth, S. I.; Gilles, S.; Giese, T.; Ablasser, A.; Hornung, V.; Endres, S.; Hartmann, G. T cell-independent, TLR-induced IL-12p70 production in primary human monocytes. *J. Immunol.* **2006**, *176*, 7438–7446.
- (63) Warshakoon, H. J.; Hood, J. D.; Kimbrell, M. R.; Malladi, S.; Wu, W. Y.; Shukla, N. M.; Agnihotri, G.; Sil, D.; David, S. A. Potential adjuvantic properties of innate immune stimuli. *Hum. Vaccines* **2009**, *5*, 381–394.
- (64) Bohnenkamp, H. R.; Papazisis, K. T.; Burchell, J. M.; Taylor-Papadimitriou, J. Synergism of Toll-like receptor-induced interleukin-12p70 secretion by monocyte-derived dendritic cells is mediated through p38 MAPK and lowers the threshold of T-helper cell type 1 responses. *Cell. Immunol.* **2007**, *247*, 72–84.



- (65) Philbin, V. J.; Levy, O. Immunostimulatory activity of Toll-like receptor 8 agonists towards human leucocytes: basic mechanisms and translational opportunities. *Biochem. Soc. Trans.* **2007**, *35*, 1485–1491.
- (66) Saruta, M.; Michelsen, K. S.; Thomas, L. S.; Yu, Q. T.; Landers, C. J.; Targan, S. R. TLR8-mediated activation of human monocytes inhibits TLLA expression. *Eur. J. Immunol.* **2009**, *39*, 2195–2202.
- (67) Shiota, T.; Yamamori, T. Regioselective Reactions of Organozinc Reagents with 2,4-Dichloroquinoline and 5,7-Dichloropyrazolo-[1,5-*a*]pyrimidine. *J. Org. Chem.* **1999**, *64*, 453–457.
- (68) Wang, K.; Herdtweck, E.; Domling, A. Cyanoacetamides (IV): versatile one-pot route to 2-quinoline-3-carboxamides. *ACS Comb. Sci.* **2012**, *14*, 316–322.
- (69) Kumar, S.; Nussinov, R. Close-range electrostatic interactions in proteins. *ChemBioChem* **2002**, *3*, 604–617.
- (70) Singh, J.; Thornton, J. M.; Snarey, M.; Campbell, S. F. The geometries of interacting arginine-carboxyls in proteins. *FEBS Lett.* **1987**, *224*, 161–171.
- (71) Kerry, P. S.; Mohan, S.; Russell, R. J.; Bance, N.; Niikura, M.; Pinto, B. M. Structural basis for a class of nanomolar influenza A neuraminidase inhibitors. *Sci. Rep.* **2013**, *3*, 2871.
- (72) Malito, E.; Bursulaya, B.; Chen, C.; Lo Surdo, P.; Picchianti, M.; Balducci, E.; Biancucci, M.; Brock, A.; Berti, F.; Bottomley, M. J.; Nissum, M.; Costantino, P.; Rappuoli, R.; Spraggon, G. Structural basis for lack of toxicity of the diphtheria toxin mutant CRM197. *Proc. Natl. Acad. Sci. U. S. A.* **2012**, *109*, 5229–5234.
- (73) Hood, J. D.; Warshakoon, H. J.; Kimbrell, M. R.; Shukla, N. M.; Malladi, S.; Wang, X.; David, S. A. Immunoprofiling toll-like receptor ligands: Comparison of immunostimulatory and proinflammatory profiles in ex vivo human blood models. *Hum. Vaccines* **2010**, *6*, 322–335.
- (74) Tanji, H.; Ohto, U.; Shibata, T.; Miyake, K.; Shimizu, T. Structural reorganization of the Toll-like receptor 8 dimer induced by agonistic ligands. *Science* **2013**, *339*, 1426–1429.
- (75) Ostinowski, Z.; Minor, W. W. Processing of X-ray Diffraction Data Collected in Oscillation Mode. *Methods Enzymol.* **1997**, *276*, 307–326.
- (76) Battye, T. G.; Kontogiannis, L.; Johnson, O.; Powell, H. R.; Leslie, A. G. iMOSFLM: a new graphical interface for diffraction-image processing with MOSFLM. *Acta Crystallogr., Sect. D: Biol. Crystallogr.* **2011**, *67*, 271–281.
- (77) Vagin, A.; Teplyakov, A. Molecular replacement with MOLREP. *Acta Crystallogr., Sect. D: Biol. Crystallogr.* **2010**, *66*, 22–25.
- (78) Emsley, P.; Cowtan, K. Coot: model-building tools for molecular graphics. *Acta Crystallogr., Sect. D: Biol. Crystallogr.* **2004**, *60*, 2126–2132.
- (79) Murshudov, G. N.; Vagin, A. A.; Dodson, E. J. Refinement of macromolecular structures by the maximum-likelihood method. *Acta Crystallogr., Sect. D: Biol. Crystallogr.* **1997**, *53*, 240–255.
- (80) Laskowski, R. A.; MacArthur, M. W.; Moss, D. S.; Thornton, J. M. Procheck: a program to check the stereochemical quality of protein structures. *J. Appl. Crystallogr.* **1993**, *26*, 283–291.